CENTRO DE INVESTIGACIÓN Y DE ESTUDIOS AVANZADOS DEL INSTITUTO POLITÉCNICO NACIONAL

UNIDAD MONTERREY

"Interacción termodinámica de especies lipídicas en sistemas de membrana multicomponente"

Tesis que presenta:

Eric Oropeza Guzmán

Para obtener el grado de:

DOCTOR EN CIENCIAS

EN

INGENIERÍA Y FÍSICA BIOMÉDICAS

Director de Tesis:

Dr. Jesús Carlos Ruiz Suárez

Apodaca, Nuevo León

Agosto, 2019

CENTRO DE INVESTIGACIÓN Y DE ESTUDIOS AVANZADOS
DEL INSTITUTO POLITÉCNICO NACIONAL

UNIDAD MONTERREY

Thermodynamics of lipid interactions in multicomponent membrane systems.

Tesis que presenta

Eric Oropeza Guzman

para obtener el grado de

Doctor en Ciencias en Ingeniería y Física Biomédicas

Director de tesis:

Dr. Jesús Carlos Ruiz Suárez

Apodaca, Nuevo León Agosto, 2019

Agradecimientos

Ninguno de los resultados obtenidos durante este trabajo hubiese sido posible sin el importante apoyo de las personas que estuvieron a mi lado durante estos años de trabajo. Agradezco en particular a mi asesor por haberme ofrecido una gran cantidad de consejos, discusiones y sobretodo disposición para que la realización de experimentos nunca se viera truncada. No puedo dejar de lado la inmensurable ayuda que me ofrecieron todos mis compañeros de laboratorio, el profesorado y en general del CINVESTAV. Gracias a todos ellos obtuve el entrenamiento necesario para realizar las diversas técnicas experimentales y teóricas que forman parte de este proyecto. Finalmente, pero no menos importante, agradezco al CONACYT por otorgarme el honor de ser miembro becario.

Table of Contents

Abstract

The thermodynamic interaction of lipid species in multicomponent membrane systems was studied with a variety of experimental techniques using multiple species of glycerophospholipids, sphingophospholipids and cholesterol. It was found that homogeneous systems can originate from binary lipid mixtures after a cyclic process of dehydration and rehydration in aqueous dispersion without the use of organic solvents. The differential scanning calorimetry scans of these samples were undistinguishable from their controls where mixtures were solubilized using an organic solvent phase. Subsequently, an optimized experimental protocol for the electroformation of micrometric membrane models (giant unilamellar vesicles) was implemented. This realization was accomplished through the development of a novel lipid film deposition technique. The protocol reduced the appearance of vesicle defects in a statistically significant manner. Finally, the phase separation properties of a well-studied ternary system were probed by inclusion of a fourth lipid component in the membrane. It was observed that a particular species of bis-phosphatidylglycerol was able to suppress the appearance of circular and coalescent domains of a liquid ordered phase in favor of stripes with presumably lower line tension.

Resumen

Se estudió la interacción termodinámica de especies lipídicas en sistemas de membrana multicomponente utilizando una variedad de técnicas experimentales. Se utilizaron diferentes especies de glicerofosfolípidos, esfingolípidos y colesterol. Encontramos que es posible preparar mezclas homogéneas de fosfolípidos mediante de deshidratación cíclica de suspensiones acuosas de liposomas, sin requerir solventes orgánicos. Los termogramas obtenidos mediante calorimetría diferencial de barrido no mostraron diferencias significativas entre muestras y controles mezclados con el método tradicional.

Posteriormente, se optimizó el proceso de preparación de liposomas gigantes por electroformación. Esto se logró mediante el desarrollo de una nueva técnica de deposición de películas lipídicas. La técnica desarrollada redujo la aparición de defectos vesiculares de forma estadísticamente significativa.

Finalmente, se estudiaron las propiedades de separación de fases en un sistema lipídico ternario mediante la inclusión de un cuarto componente lipídico. Se observó que una especie particular de bisfosfatidilglicerol fue capaz de suprimir la formación de dominios líquido-ordenados y en su lugar se observaron dominios lineales con aparente menor tensión de línea.

Introduction.

Compartmentalization is a central concept in our understanding of cellular structure and function (Witzany, 2016). The very constitution and preservation of a cellular unit is dependent on the existance of a stable boundary that defines its spatial location, contains its molecular constituents and helps to counteract the dispersive effects of entropy production. Since water is the only medium where cellular life can exist, such stable boundary could only be created by molecular amphiphiles that are effectively adsorbed into the interface, i.e. surface-active agents. Amphipathic lipids are therefore the central subject of this work. The findings from these experiments are described within a thermodynamical framework to make sense of the observables.

In the case of multicomponent membrane systems, like biological membranes, diverse phenomena may emerge and be studied both phenomenologically and quantitatively. Several functions of the living cell are directly related to the thermodynamical properties of its membranes, ranging from environmental sensing and adaptation, signal regulation, molecular transport and morphological transformations.

In this work, particular attention was devoted to the ongoing debate concerning the mechanistic description of compositional heterogeneities on the plasma membrane that may bestow it with sub-compartmentalization properties and the consequent parallelization of its biological processes. In the process, we developed technical optimizations to previously established protocols in the field that allowed us to work on a cleaner and more robust experimental setup.

General concepts

Following is a brief description of the elemental definitions pertinent to the physicochemical study of lipids and its phases.

Chemical classification

Glycerophospholipids

Characterized by a central glycerol moiety that is covalently attached to acyl chains through ester bonds in up to two of its carbon atoms. The third carbon atom is attached to a phosphate

residue. This configuration constitutes the simples form of glycerophospholipid called phosphatidic acid. Additional residues attached to the phosphate moiety help distinguish between different subclasses of glycerophospholipids, namely:

- Phosphatidylcholine
- Phosphatidylethanolamine
- Phosphatidylserine
- Phosphatidylglycerol
- Phosphatidylinositol
- Bis-phosphatidylglycerol

Sphingophospholipids

In this class of lipids, a central serine molecule replaces glycerol as the backbone of the molecule. The serine moiety condensates with an acyl chain to form sphingosine, which can be bonded to a second acyl chain in its amino group to form ceramide. Just like the preceding class, sphingophospholipids are distinguished by the type of acyl chains and the different residues bonded in the headgroup region, just like sphingomyelin, which is the product of ceramide and a phosphocholine or phosphoethanolamine molecule.

Sterols

Also known as steroid alcohols, it's a group of steroids from which we study just one member, cholesterol. Like the rest of the steroids, cholesterol is derived from the same four-ringed structure made from three cyclohexane rings and one cyclopentane ring all formed from the condensation of isoprene subunits in their common precursor lanosterol.

Phase classification

Following the nomenclature described in (Marsh, 2013), an upper case letter describes the long-range organization of a lipid phase, and a lower-case Greek suffix is used to characterize the conformation of the acyl chains. Besides, roman numerals differentiate the content of the structural elements in the phase, where these can be distinguished topologically.

Long-range organization

- L, one-dimensional (lamellar).

- H, two-dimensional hexagonal.
- P, two-dimensional oblique or centered.
- Q, three-dimensional, cubic.
- R, three-dimensional, rhombohedral.
- M, disordered (micellar).

Short-range chain order

- α, disordered (fluid).
- β, partly ordered (elongated), untilted.
- β', partly ordered (elongated), tilted.
- δ, partly ordered (helical).
- C, crystalline.

Content of structure element

- I, oil-in-water.
- II, water-in-oil.

When focusing on the study of the lamellar phase, several terms and acronyms have been developed in the literature under the umbrella term of *liposomes*, which are defined as lipid vesicles with an aqueous core and suspended in an aqueous dispersion (Akbarzadeh et al., 2013). This type of classification rather focuses on the morphological characteristics of the vesicle unit, instead of the lipid phase.

- MLV, multilamellar vesicle
- MVV, multivesicular vesicle
- GUV, giant unilamellar vesicle
- LUV, large unilamellar vesicle
- SUV, small unilamellar vesicle

The discrimination of size in this classification is rather arbitrary. Working definitions can nonetheless be delimited, where *giant* is understood as: above the diffraction limit of optical microscopy; *small* as: sub-optical and produced with sonication methods; and *large* describes sub-optical liposomes produced with non-sonication methods like extrusion.

Phase behavior

Polymorphism

The previously enlisted phases can display both lyotropic or thermotropic mesomorphism. In the absence of water, all the lipid is in the crystalline phase (L_C). Lipid-water systems on the other hand, have a lyotropic transition from the crystalline phase to any of the other phases, although the appearance of disordered and especially non-lamellar phases requires a thermotropic transition too. Lipid-water systems derive their structure to the large free energy of interaction between water and lipid molecules. This so-called hydrophobic effect is large enough to counteract the entropic penalty of lipid self-assembly. After the initial assembly, formation of bilayers and curved membranes whether in closed discrete vesicles or any of the non-lamellar phases is guided now by the energy of bending and spontaneous curvature (Guida, 2010).

A spontaneous curvature on a lipid membrane is a consequence of the molecular packing parameter (a quantitative relationship between the lipid monomer geometries), and it is responsible for the discrimination between normal oil-in-water (type I) and inverse water-in-oil (type II) phases (Antonietti & Förster, 2003). In this way, single-chain lipids or lipids with a very large headgroup have a small packing parameter that favor the formation of oil-in-water (type I) phases. On the contrary, water-in-oil (inverse, type II) phases are usually favored in rather dehydrated systems of lipids with large packing parameters.

Thermotropic transitions

Increasing the temperature of a lipid-water system in excess water produces a series of phase transitions between distinct lamellar phases. For medium-chain phosphatidylcholines and phosphatidylglycerols, the L_C crystalline phase is seen to convert into a metastable $L_{\beta'}$ gel tilted phase at a point called the subtransition temperature T_s. Other types of lipids like phosphatidylethanolamines transition into an untilted phase called L_β. Some phospholipids transition from the gel phase into the $P_{\beta'}$ ripple phase at the pretransition temperature T_p. And at an even higher temperature (the main transition temperature T_m), the $P_{\beta'}$ is seen to convert into the L_α liquid-disordered (fluid) phase. Increasing the lipid chain length elevates their melting point but also reduces the temperature range where the $P_{\beta'}$ phase can exist, until the T_p and T_m transition temperatures merge (Heimburg, 2007).

The main transition temperature T_m is known to be a highly cooperative event, yielding very narrow heat capacity c_p peaks in calorimetry scans. The cooperativity of the transition is dependent on the interfacial energy (i.e. line tension) between lipids in the gel-phase and the fluid-phase. Such tension comes from the elevated entropic and enthalpic cost of exposing hydrocarbon chains to water. Exposure derives in broken hydrogen bonds and water molecule organization around non-polar lipid areas.

Phase coexistence and phase separation

Simple lipid-water systems of only one lipid species can show phase coexistence according to the Gibbs phase rule (i.e. F = C – P + 2). The rule is derived from the Gibbs-Duhem equation and determines the number of independent variables available at equilibrium. In excess water and constant pressure there is only one degree of freedom because the fully hydrated lipid can be taken as the only component of the system. After full lipid hydration, excess water taken as an extra component will readily separate into its own phase and become inconsequential to the Gibbs phase rule. This means that phase-coexistence can only occur at a fixed temperature (F = 0), the main transition temperature.

However, biological membranes are composed of hundreds of different lipid species. Regular solution theory considers multicomponent systems as having a purely enthalpic contribution to the non-idealities in the free energy of mixing (Marsh, 2013). In this framework, the interaction energy of a binary lipid mixture can be modeled using the Bragg-Williams parameter ρ as the proportionality constant between the free energy of mixing and the product of the molar fractions of lipids A in B in the mixture:

$$\Delta G^{E}_{mix} = \rho X_B (1 - X_B)$$

This proportionality constant would be determined by an arithmetic comparison (interaction parameter) of the strength of interaction energies present in each possible pair of the two lipids (i.e. A-B, A-A, B-B):

$$\rho = z(u_{AB} - 0.5(u_{AA} + u_{BB}))$$

for z nearest lipid neighbors in the bilayer lattice and can be derived using experimental techniques.

Regular solution theory, however, does not consider the free energy arising from domain interfaces. Pair-wise interaction parameters are already known to be not entirely independent on system composition and are most obviously dependent on system temperature due to the hydrophobic effect on the melted hydrocarbon chains. Melted chains have a shortened effective length in comparison to their ordered counterparts, and interfacial tension is generated along the bidimensional plane of the membrane so that phase separation would ensue. If one should also take into account non-idealities in the entropy of mixing, the interaction parameter should be obtained by a statistical treatment (e.g. Monte-Carlo simulation) in replacement of the regular solution approximation that considers the entropy of mixing to behave ideally.

In the end, phase separation, at different correlation lengths will depend on the interplay between line tension and temperature but an important distinction is automatically made by this correlation length. A lipid-water system can contain fluctuations in composition and state that promote small compositional heterogeneities but do not necessarily correspond to phase coexistence which necessarily requires stable equilibrated separation. In the case of critical fluctuations, the Gibbs phase rule cannot be applied to describe the system (Heimburg, 2007).

Dynamic properties

Phospholipid molecules within the hydrated phases can display, lateral, transverse (flip-flop) and rotational diffusion.

Lateral diffusion

As a translational random movement along the bilayer plane of a lamellar phase, this type of diffusion is described by the partial differential equation:

$$\frac{\partial P}{\partial t} = D_T \cdot \nabla^2 P$$

where the function $P(r,t)$ is the time-dependent probability of location at a point r for a lipid molecule. Therefore, the translational diffusion coefficient D_T is the proportionality constant between the partial time derivative of this probability function and its Laplacian.

The coefficient D_T is also related to the mean square lateral displacement of the molecule by the Einstein equation for Brownian bidimensional motion $\langle r^2 \rangle = 4D_T\tau$.

Experimental values for D_T in membranes are usually obtained through fluorescence recovery after photobleaching (FRAP) techniques which yield values in the range of 1-10 $\mu m^2 s^{-1}$ for the L_α phase.

Miscibility

Mixtures of lipids show different miscibility within the membrane that depends on different factors. For binary mixtures, one of the most important parameters is the difference in main transition temperature of the lipid species. Miscibility of lipid species can be classified as (Silvius, 1986):

- P, perfect: mixing is ideal and there is no broadening of the main transition peak.
- VH, very high: ideal mixing where the resulting transition peak is broader than those of the pure components.
- H, high: slightly non-ideal mixing where the resulting transition peak is markedly broader.
- M, moderate: non-ideal mixing where the *solidus* curve is not horizontal (i.e. gel phase immiscibility) over any significant range of compositions.
- L, low: non-ideal mixing where the *solidus* is essentially horizontal over a range of compositions that span 20-50% of the mole fraction (horizontal) axis on the phase diagram.
- VL, very low: non-ideal mixing where the *solidus* is essentially horizontal over more than 50% of the mole fraction axis.

Binary phase diagrams can be constructed from the melting properties of single-species lipid water systems and experimental techniques that allow the identification of the existing phases (e.g. X-ray diffraction). In such diagrams, lipid phases are delimited by variations in temperature and mole fraction of a lipid species with respect to the total lipid mass. Given the extra degree of freedom that the second lipid component provides, the Gibbs phase rule now allows two-phase coexistence at different values of temperature or composition and a single point of three-phase coexistence. A curve that traces the boundary between the gel

phase region and the region of gel-fluid coexistence in this phase diagram is called *solidus*, whereas its analog between the gel-fluid coexistence and the fluid phase regions is called *liquidus*.

The interaction parameter ρ between two lipid species depends on their pair-wise interaction energies and is given by

$$\rho = z\left(u_{AB} - \frac{1}{2}(u_{AA} + u_{BB})\right)$$

for z lipid nearest neighbors, so that $\rho = 0$ characterizes ideal mixing (vanishing enthalpy of mixing). On the contrary, a non-zero interaction parameter will characterize a mixing pattern that is different from a random distribution, whether there are net attractive interactions between unlike species ($\rho < 0$) or cluster formation of like species ($\rho > 0$) (P. F. F. Almeida, 2009).

Bilayer-bilayer interactions

The net interbilayer pressure in a lipid-water system can be characterized by the balance of attractive and repulsive microscopic and macroscopic forces that will determine an interbilayer spacing at equilibrium (Marsh, 2013):

1. Van der Waals: a relatively long-ranged attractive force between the bilayer surfaces characterized by the effective London-Hamaker coefficient.
2. Hydration force: an exponentially decaying short-range repulsion (2-3 Å) that arises from water polarization at the bilayer surface.
3. Fluctuation force: another exponentially decaying repulsion that comes from thermally excited bending fluctuations of the lipid bilayer that become suppressed by close apposition.
4. Electrostatic force: a much longer-ranged (than the van der Waals attraction) repulsive pressure arising from the excess osmotic pressure of the ions at the midplane between bilayers.

Chapter I. Cyclic dehydration of aqueous liposomal dispersions.

This chapter is essentially a challenge to the traditional protocol for the experimental preparation of a lipid mixture for the eventual production of a membrane model that imitates the multicomponent nature of biological membranes. On our way to find a straightforward alternative, we developed and tested a hypothesis for the particular case of binary glycerophospholipid mixtures, using differential scanning microcalorimetry as the experimental technique of sample comparison (Oropeza-Guzman & Ruiz-Suárez, 2018).

I.1 Introduction

Traditional lipid mixing has always relied on the use of suitable organic solvents for the dispersion and combination of lipid components (Bangham, 1968). Every lipid possesses a variable degree of solubility in different organic phases like acetone, short-chain alcohols, chlorinated solvents, n-alkanes, diethyl ether and combinations of these in different ratios.

In the case of a simple system with one lipid and one solvent species, said solubility will depend on the pairwise interaction of solvent-solute molecules. However, additional lipid or solvent species in the mixture will actively modify the solubility of even previously soluble components (Dervichian, 1964). In the most time-consuming scenarios, each lipid component must be dispersed separately in an appropriate solution of organic solvents. These single-lipid solutions are then mixed in the desired proportion, hoping that the whole will not unmix and result in a heterogeneous film after solvent removal.

Solvent removal is the final step of the sample preparation where traces of solvent are usually removed after a lengthy exposure under vacuum conditions. Changing the proportion of any of the lipid components could in some cases compromise the stability of the mixture since different species may possess entirely different partition coefficients in the solvent components. The final consequence is that each lipid ensemble needs experimental characterization and fine-tuning of an appropriate solvent combination, which needlessly complicates the preparation process.

On the other hand, some of the organic solvents used for phospholipid solubilization are cataloged as undesirable due to their potential for human toxicity and environmental damage (Dwivedi, 2002). Pharmaceutical liposome formulations that make use of these solvents in any step of the preparation process are regulated by the FDA and the US Pharmacopoeia

(B'Hymer, 2003). In addition, due to the elevated vapor pressure of organic solvents, their precise measuring can become cumbersome and large quantities tend to be used to average-out volumetric errors in their handling.

Some of these reasons have motivated the development of 'greener solvents' with better environmental, health and safety (EHS) characteristics (Capello, Fischer, & Hungerbühler, 2007). Alternative solvents remain a current topic of research with significant economic implications (Clarke, Tu, Levers, Bröhl, & Hallett, 2018).

I.2 Justification

Several techniques using different protocols for liposome preparation have been proposed, including reverse phase evaporation (Cortesi et al., 1999), rapid injection (Batzri & Korn, 1973), detergent depletion (Brunner, Skrabal, & Hausser, 1976), supercritical fluids (Otake, Imura, Sakai, & Abe, 2001), membrane contactor (Charcosset, El-Harati, & Fessi, 2005), and the polyol dilution or heating method (Mozafari, Reed, Rostron, Kocum, & Piskin, 2002). However, no technique has been previously developed that completely avoids the use of organic solvents, cosolvents or additives to mix phospholipids.

In this work, we present a technically simple method to prepare mixed phospholipid films, that avoids the time-consuming process of characterizing an appropriate solvent combination for each case, since it only employs deionized water in every scenario. The method is based on the repeated dehydration and rehydration of a lipid-water system that contains the phospholipid species to be mixed. We see that the ability of the method to produce a liposomal population with equivalent compositional homogeneity to that of the traditional technique, is a consequence of two physicochemical properties of phospholipids, namely the thermodynamic interaction parameter and the lateral diffusion coefficient in the lamellar phase.

I.3 Hypothesis

We set out to test weather the proposed cyclic dehydration protocol applied to an aqueous phospholipid dispersion can produce a homogeneous binary mixture that renders a single, well-defined peak on the calorimetric scan.

I.4 Objective

The general objective is to develop an experimental technique for lipid mixing that completely avoids the use of organic solvents, cosolvents or additives.

I.5 Research methodology

I.5.1 Materials

The following reagents were purchased in dry powder form from Avanti Polar Lipids (Alabaster, USA) and used as received:

- 1,2-dimyristoyl-*sn*-glycero-3-phosphocholine (DMPC)
- 1,2-dipalmitoyl-*sn*-glycero-3-phosphocholine (DPPC)
- 1,2-dipalmitoyl-*sn*-glycero-3-phospho-(1'-*rac*-glycerol) (sodium salt) (DPPG)
- 1,2-dipalmitoyl-*sn*-glycero-3-phosphate (sodium salt) (DPPA)
- 1,2-dipalmitoyl-*sn*-glycero-3-phosphoethanolamine (DPPE)
- 1,2-dipalmitoyl-*sn*-glycero-3-phospho-L-serine (sodium salt) (DPPA)

The following reagents were purchased from Sigma-Aldrich (Toluca, México):

- Chloroform (anhydrous, ≥99%, with 0.5-1.0% ethanol as stabilizer)
- Methanol (anhydrous, 99.8%)
- Dichloromethane (ACS reagent, ≥99.5%, with 50 ppm amylene as stabilizer)

Twice distilled water was treated with the Milli-Q IQ 7000 Ultrapure Water System from Merck Millipore México (Naucalpan de Juarez, México) prior to use. Phosphate buffered saline tablets from Sigma-Aldrich (1 tablet in 200 mL water) were used to obtain a 137 mM NaCl, 2.7 mM KCl and 10 mM PBS solution with pH 7.4 at 25 °C.

I.5.2 Methods

The assayed lipid mixtures were:

- DMPC/DPPC (50/50) mol %
- DPPC/DPPA (50/50) mol %
- DMPC/DPPG (50/50) mol %

- DPPS/DPPE (50/50) mol %.

Four micromoles of each phospholipid in powder form were weighed inside a clear scintillation vial using an analytical balance (OHAUS Explorer EX224). The balance was calibrated before each use using an analytical weight set certified by Troemner (Weight ID Number 4000017899 – Certificate Number 852839) by testing with NIST Traceable Reference Standards (NIST Test Number 822-275872-11). Variable volume manual pipettes (Eppendorf Reference 2) were checked to dispense within manufacturer reported tolerances before each working day, using the gravimetric tool programmed into the OHAUS Explorer EX224 balance.

The vial containing the lipid powder was preheated for 15 min at the working temperature (i.e., 10 °C above the main transition temperature of the highest melting lipid in the mixture). Double distilled deionized water (100 μL) at the same temperature was added to the dry lipid powder inside the vial using the technique recommendations of the pipette manufacturer.

The resulting lipid paste was stirred at 200 rpm with a small magnetic bar while keeping the vial above a lab stove at the same temperature. The vial was maintained on the stove for about 12 minutes until the lipid was dried to the naked eye. After drying, deionized water was added again, and this cycle was repeated three times. After three cycles of drying and rehydration, phosphate buffered saline (137 mM NaCl, 2.7 mM KCl and 10 mM PBS, pH 7.4) was added to the dry mixed lipid film to obtain multilamellar vesicle samples with a total lipid concentration of 5 mM.

For the controls, multilamellar vesicle dispersions were prepared with the solvent evaporation method using the same four mixtures. Each phospholipid was weighed in a separate vial, and the appropriate organic solvent added to solubilize the lipid according to the following table:

Phospholipid	**Solvent components**	**Solubilization temperature**
DPPC	Chloroform	Room temperature
DMPC	Chloroform	Room temperature

DPPA	Chloroform/methanol/dichloro-methane (2:1:1 v/v/v)	35 °C
DPPE	Chloroform/methanol (2:1 v/v)	35 °C
DPPG	Chloroform/methanol (2:1 v/v)	Room temperature
DPPS	Chloroform/methanol (2:1 v/v)	35 °C

Table I.1 Solubilization parameters for each phospholipid used in the mixtures.

After solubilizing each phospholipid, equimolar amounts were mixed in the same vial. The organic phase was then removed in a fume hood with a nitrogen stream until dry to the naked eye. The mixed dry lipid film was kept under vacuum for 60 minutes to remove remaining solvent traces. Afterward, phosphate buffered saline (137 mM NaCl, 2.7 mM KCl and 10 mM PBS, pH 7.4) was added to reach a final total lipid concentration of 5 mM.

I.5.3 Vesicle processing and characterization

Multilamellar vesicles were processed the same way independently of the mixing method. A total of 1 mL of vesicles (5 mM) was loaded into a syringe and extruded 15 times using the Avanti Mini Extruder that was preheated to the working temperature. A polycarbonate membrane with a pore size of 100 nm was used. The quality of the extrusion products was checked for all samples using dynamic light scattering with a Zetasizer Nano ZS equipment (Malvern, Worcestershire, UK).

After extrusion, all the samples were equilibrated to room temperature right before calorimetric analysis. Samples were loaded into a differential scanning calorimeter (Nano DSC, TA Instruments). After 800 seconds of equilibration time, a heating scan was performed at a rate of 1 °C/min and a cell pressure of 3 atmospheres.

I.6 Results and discussion

Figure I.1 shows representative scans of samples and controls after baseline subtraction. The obtained curves are characteristic of extruded unilamellar suspensions of liposomes, having a relatively broad transition half-width with a small cooperative unit size, which results in much lower maximum heat capacity values in comparison with those of multilamellar systems. Main transition temperature T_m and enthalpy change ΔH were characterized from each of these scans.

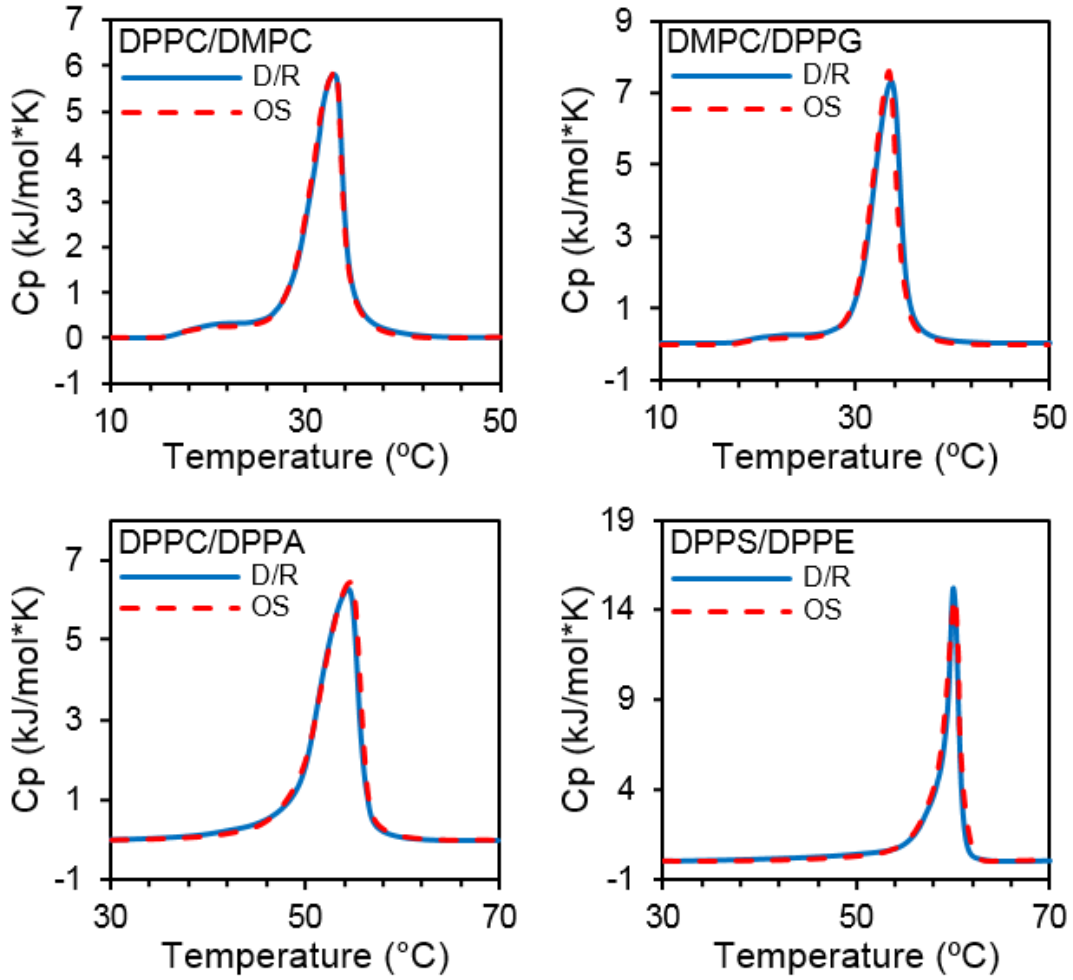

Figure I.1 Molar heat capacity as a function of temperature for the four assayed mixtures using the dehydration/rehydration (D/S) method vs controls using organic solvent (OS) evaporation. Note the axis scaling in each box.

The following table shows the arithmetic mean and standard deviation of the calorimetric parameters from **Figure I.1** using three independent experiments from each mixture and mixing method. Bragg-Williams parameters are taken from (Marsh, 2013) and (Wydro, 2011):

DMPC/DPPC (50/50) mol %	**ρ_F (-0.01 to 2.84) kJ mol^{-1}**	
	T_m (°C)	ΔH (kJ/mol*K)
Organic solvent evaporation	33.05 ± 0.15	28.37 ± 0.79
Dehydration/rehydration	32.85 ± 0.15	29.39 ± 0.74
DPPA/DPPC (50/50) mol %	**ρ_F (-5.79 to 3.30) kJ mol^{-1}**	
	T_m (°C)	ΔH (kJ/mol*K)

Organic solvent evaporation	54.64 ± 0.18	35.60 ± 0.74
Dehydration/rehydration	54.56 ± 0.15	34.59 ± 0.73
DMPC/DPPG (50/50) mol %	**ρ_F (-4.79) kJ mol^{-1}**	
	T_m (°C)	ΔH (kJ/mol*K)
Organic solvent evaporation	33.47 ± 0.12	28.07 ± 0.78
Dehydration/rehydration	33.65 ± 0.14	29.09 ± 0.76
DPPE/DPPS (50/50) mol %	**ρ_F (-0.35 to -0.01) kJ mol^{-1}**	
	T_m (°C)	ΔH (kJ/mol*K)
Organic solvent evaporation	59.90 ± 0.07	38.92 ± 0.58
Dehydration/rehydration	59.97 ± 0.04	38.30 ± 0.66

Table I.2. Calorimetric parameters for each phospholipid mixture using the compared methods of lipid mixing. The range of published values for the fluid-phase Bragg-Williams parameter ρ_F is enlisted next to the mixture components.

We can see that the resulting thermograms for the dehydration/rehydration method show almost identical curves than those obtained from liposome samples prepared with the traditional organic solvent evaporation technique. This result suggests that, for these four mixtures, the selected process of phospholipid mixing shows no differential effect on the compositional homogeneity of the system.

Whenever a lipid mixture with a cooperative melting transition contains an random molecular distribution of its components (i.e. ideal interaction), then a single, well-defined endothermic peak can be obtained by thermal analysis (Krisovitch & Regen, 1992). The same calorimetric fingerprint could be applied to mixtures with a negative Bragg-Williams parameter, since they will favor a chemical composition with checkerboard pattern of lipid A and lipid B in the mixture. On the contrary, binary mixtures with a positive parameter can potentially yield more than one endothermic peak that will signal like-lipid cluster formation (Silvius, 1986).

According to the enlisted values for the Bragg-Williams parameters in **Table I.2**, neither the DMPC:DPPC mixture nor perhaps the DPPA:DPPC combination should yield a single endothermic peak due to the repulsive interaction of unlike lipid molecules. Since all the mixtures were equimolar, the possible dependence of the interaction parameters on the system chemical composition can be neglected. However, we see that all the results in **Figure**

I.1. show a single peak. The most likely conclusion is that these lipid mixtures can be trapped in a metastable state by a proper solubilization process, but also by a cyclic dehydration of their aqueous dispersions (since the resulting peaks are identical). In the thermodynamical context, chemical composition is a state function and must therefore have a path independent integral. The chosen mixing process shouldn't affect the final result.

From a practical standpoint, this argument would also mean that different lipid mixtures could be prepared by a standardized method. We decided to take advantage of this observation and hypothesized that these lipid mixtures should be able to reach compositional homogeneity in the medium with the best EHS characteristics that there is (i.e., water), without the need to be dissolved in proper solution beforehand. However, upon direct hydration with an aqueous medium, and due to their amphiphilic character, phospholipids spontaneously arrange into a series of closed concentric bilayer structures (i.e., multilamellar vesicles) that restrict their ability to create a homogeneously combined system. For the phospholipid molecules to be able to distribute more randomly, there must be a way to exchange phospholipid molecules between separate bilayers within the lipid-water system. This part is where the dehydration step becomes useful.

The optimal number of dehydration/rehydration cycles was determined empirically for the DMPC/DPPC mixture, since is the one with the most unfavorable Bragg-Williams parameter. In this mixture, extruded liposomes obtained from dried lipid films with less than three cycles of dehydration/rehydration were prepared and analyzed with DSC. The resulting curves are depicted in **Figure I.2**. As expected, simple direct hydration of mixed lipid powders is unable to produce a homogeneous system, but each dehydration/rehydration cycle progressively contributes to create the metastable state and merge the two endothermic peaks that initially correspond to each one of the pure lipid species.

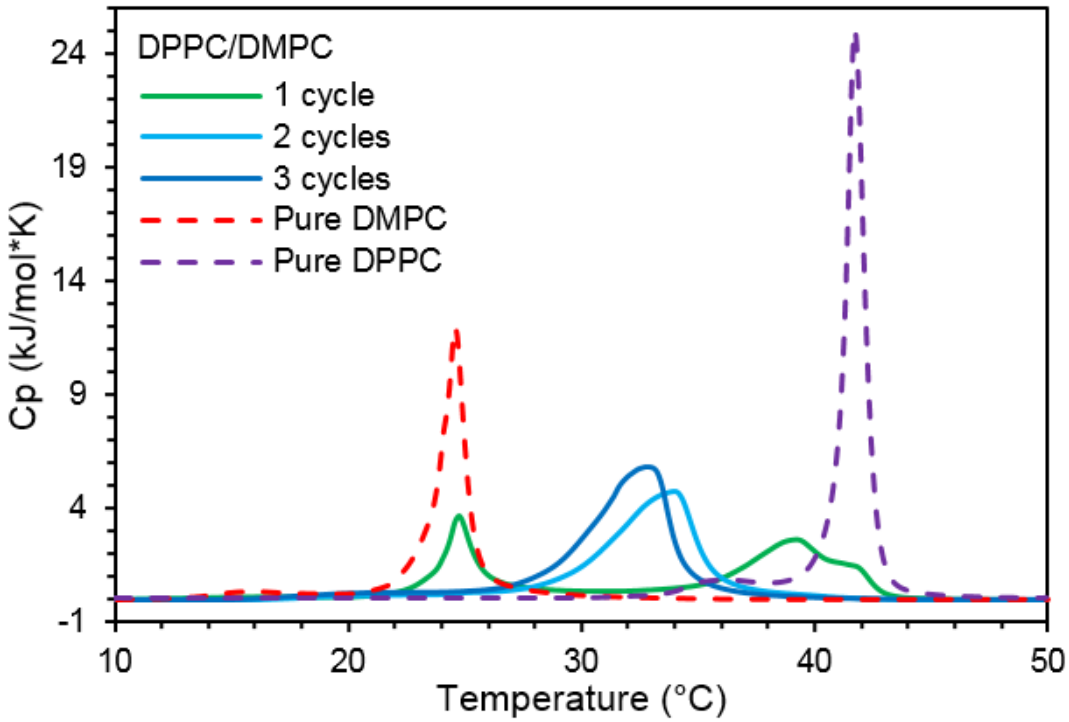

Figure I.2. Molar heat capacity as a function of temperature for the DMPC/DPPC mixture using the dehydration/rehydration method. Discontinuous lines show the thermograms of each pure lipid species separately. The curve corresponding to '3 cycles' is the same that the one depicted in the top-left corner of **Figure I.1.**

During the drying phase of each mixing cycle, the bilayers in the system intimately approximate as the water content is reduced. As described in the general introduction of this thesis, there are several forces that contribute to an increased interbilayer pressure when two lamellar surfaces approach each other. These forces should conspire to keep lipid molecules from accessing all the bilayers in the system; however, published experiments point out to the conclusion that beyond a threshold approximation value around 1 nm, fusion between two bilayer surfaces does occur (Helm, Israelachvili, & McGuiggan, 1989). The bilayers are thought to overcome the repulsive forces between them via highly localized fluctuations in the membrane integrity. These instabilities promote the hydrophobic attraction between the internal alkyl chains of the apposed membranes, resulting in hemifusion (i.e., transmonolayer contact) and lipid mixing.

Theoretical models of intimate bilayer apposition seem to corroborate this finding using molecular dynamics simulations (Ohta-Iino et al., 2001). These authors show that even when

all the phospholipid molecules in the bilayers are saturated with water (i.e. repulsive hydration force), the proximity to each other seems to induce a reorientation of the alkyl chains. Some of the chains were seen to lie parallel to the membrane plane or even to protrude out of the bilayer. Alkyl chain reorientations occurred almost instantaneously (within several tens of picoseconds) after the two membranes approached each other.

In our experiments, close apposition between bilayers certainly occurs during the evaporation of the aqueous phase, but the time period where the threshold apposition value is reached before all the water phase has evaporated could be potentially short. It is only in this time frame where lateral diffusion of phospholipid molecules between neighboring vesicles in the system would reach a random distribution of components.

Experimental data from published pulse field gradient (PFG) NMR measurements of lipid self-diffusion (Lindblom, Orädd, & Filippov, 2006), and FRAP methods using fluorescent probes (Vaz, Clegg, & Hallmann, 1985), (P. F. F. Almeida, Vaz, & Thompson, 1992), report that the phospholipid lateral diffusion coefficient in lamellar phases of DMPC or DPPC is always above 15 $\mu m^2 s^{-1}$ for temperatures around 60 ºC. With such values in mind, we saw that we required up to three dehydration cycles to obtain a homogeneous lipid distribution for the "most unfavorable" mixture (i.e. DMPC/DPPC).

We paid particular attention to the mixture using DPPS and DPPE since the latter lipid has a very stable L_c phase that cannot be dispersed in deionized water, even when the temperature of the system is above the temperature of its melting transition. The finding that a mixture with this lipid can be prepared by our proposed method implies that the energy of interaction between DPPS and DPPE molecules, in the aqueous lamellar phase, is lower than the energy of interaction of DPPE in the dry crystal phase, which may account for the aqueous solvation of otherwise insoluble DPPE crystals.

I.7 Conclusion

We proposed a standardized lipid mixing method that uses deionized water as the only mixing agent in every case, avoiding the need to characterize an appropriate organic solvent combination for different sets of lipid components. After three cycles of drying and

rehydration, the DSC characterization of our samples showed equivalence with the traditional solvent evaporation technique.

From a technical point of view, this alternative provides a valuable advantage over the traditional method, since it simplifies and speeds up the preparation process. It also benefits from requiring only simple laboratory tools without the need for high-pressure equipment or special installations. From the environmental health and safety standpoint, we are confident that the technique can contribute to the interest that the research community has expressed on the implementation of sustainable chemical practices (Horváth, 2018), or situations where organic solvent use is closely regulated.

We see that this technique constitutes a fast, solvent-free and technically simple standard method for mixing miscible lipids, especially useful in situations where several iterations must be made to study the effect that the titration of a lipid constituent has on the physicochemical properties of a mixed system. Moreover, it can be implemented as a complement to previously published techniques that make use of alternative solvents with reasonable EHS profiles when the need to incorporate components with negligible solubilities in aqueous solutions arise. An example of such scenario would be the sterol-containing ternary mixtures. Although Bragg-Williams parameters are also negative for the DPPC-Chol and SM-Chol pairs, a fact that explains their association in the liquid-ordered phase (P. F. Almeida, 2011), cholesterol crystals are highly stable and virtually insoluble in pure water (Haberland & Reynolds, 1973). Hence, our proposed technique would not be applicable in these cases.

Chapter II. Concentric deposition of liposomal droplets for thin film preparation.

The need to explore thermodynamic lipid interaction by optical tools led us to implement an experimental setup for the preparation of giant unilamellar vesicles (GUV). However, we soon realized that the state-of-the-art techniques had certain disadvantages like the appearance of a considerable fraction of lipid defects in vesicle samples. After careful overview of the dynamics involved in the evaporation droplets for thin film formation, we saw an opportunity window to leverage the well-known coffee ring effect in our favor. This finding led us to develop an optimized protocol of GUV preparation.

II.1 Introduction

Giant unilamellar vesicles (GUV) are a tool of paramount importance to membrane biophysics research. They have been employed to study a broad set of phenomena including mimetic cell motility (Bartelt, Steinkühler, Dimova, & Wegner, 2018), lateral molecular difusión (Tingting Wang, Ingram, & Weisshaar, 2010), confined protein synthesis (Nishimura et al., 2012), or lipid membrane viscosity (Tabaei et al., 2016), to name a few.

Future studies that hope to also take advantage of this extremely dynamic tool would benefit from a GUV preparation procedure that could yield a high number of defect-free unilamellar vesicles, preferably without the use of any organic solvent or potentially contaminating additive during the preparation process.

To that end, several GUV fabrication techniques have been developed and reviewed over the years (Bagatolli, Parasassi, & Gratton, 2000; Patil & Jadhav, 2014; Rideau, Dimova, Schwille, Wurm, & Landfester, 2018; Walde, Cosentino, Engel, & Stano, 2010). Among them, the microfluidic on-chip methods have achieved the highest success in terms of encapsulation efficiency, high throughput, and vesicle size monodispersity (Deshpande & Dekker, 2018). Yet, a significant drawback in these methods is the need to create an organic solvent phase that cannot be entirely removed, as well as having access to the specialized equipment necessary to fabricate and operate the microfluidic chip.

Therefore, thin-film-based methods remain the most frequently used in GUV preparation. Amid these methods, electroformation is by far the most popular in the literature, since it produces an uncontaminated sample with a relatively narrow dispersity profile (Rideau, Wurm, & Landfester, 2019). After more than three decades in use, electroformation has been

optimized for use in a wide variety of experimental scenarios, and it is currently being employed in the construction of advanced synthetic protocell systems (Lee et al., 2018).

II.2 Justification

Despite years of experience and remarkable successes, current electroformation protocols generate samples with vesicle defects, which are defined as lipidic structures that make a giant vesicle differ from an isolated unilamellar vesicle (Rodriguez, Pincet, & Cribier, 2005). These defects can comprise lipid aggregates, tethers, or smaller vesicles that are bound to the main vesicle or get trapped inside it. In this study, we chose to optimize the electroformation protocol by focusing on the lipid film deposition process, confirming that it is the most important step affecting the quality of the electroformed GUV sample (Angelova & Dimitrov, 1986).

Previous attempts to control the thickness and organization of lipid films have been reported in the literature. In 2005, Estes & Mayer were clearly aware that the traditional drop-casting of lipid organic solution over an indium-tin oxide (ITO) substrate produces a lipid film of variable thickness (Estes & Mayer, 2005). Only some areas the resulting film are suitable for the appearance of clean GUVs, while others are too thin or too thick. Instead, they proposed a lipid coating technique where the organic solution was spread with the help of a rotary platform, successfully obtaining more uniform films. They recognized nonetheless, that their spin-coating technique required around 15 times more lipids per substrate unit area than the traditional drop-casting.

In 2009, Le Berre et al. reported experiments using a more elaborate receding meniscus apparatus to cast lipid films at different speeds over a solid substrate with controlled temperature that also included vapor aspiration (Le Berre, Chen, & Baigl, 2009). They used a concentrated solution of DOPC in *n*-octane (20 mg/mL) and managed to prepare highly uniform films within the Landau-Levich regime of meniscus receding speeds.

Meanwhile, other researchers experimented with the use of aqueous liposome suspensions instead of lipids in organic solutions to deposit multilayer films (Pott, Bouvrais, & Méléard, 2008). Using polarized light microscopy and small angle X-ray measurements they showed that casting liposomal droplets resulted in macroscopically oriented membranes

right after water evaporation. The obtained GUV samples from these types of films led them to conclude that electroformation works better with aqueous rather than organic solvent depositions.

Additionally, it had been shown that film deposition using organic solutions of cholesterol-containing lipid mixtures can result in artifactual demixing and the appearance of X-ray diffraction intensity profiles compatible with the presence of anhydrous cholesterol crystals on the films (Huang, Buboltz, & Feigenson, 1999).

Even when aqueous liposomal deposition had improved the quality of GUV samples, a critical downside remained. Any material suspended in a sessile drying droplet with a pinned contact line will be carried to its periphery and form a ring-like stain. This phenomenon is named the coffee ring effect (CRE) and was seminally described by (Deegan et al., 1997). After systematic experimentation, they observed that the CRE was insensitive to an ample range of substrates, solvents, solute sizes, volume fractions, and environmental drying conditions (Deegan, 2000; Deegan et al., 1997, 2000).

Several studies have reported the presence of the CRE after evaporation of sessile droplets of liposome suspensions (Adams, Toner, & Langer, 2008; González-Gutiérrez, Pérez-Isidoro, Pérez-Camacho, & Ruiz-Suárez, 2017; Kočišová, Antalík, & Procházka, 2013; Kočišová, Petr, Šípová, Kylián, & Procházka, 2017; Kočišová & Procházka, 2011). It is understood that this effect will inexorably produce a multilayer film of variable thickness, where most of the lipid mass ends up concentrated at the edge of the ring-like stain. The consequence of this distribution is a higher frequency of vesicle defect appearance in the electroformed GUV sample.

Liposomal CRE has been observed even in smooth substrates with relatively small contact angle hysteresis (i.e., weak contact line pinning) (Kočišová et al., 2017). Likewise, these ring-like stains show insensitivity to variations in chemical lipid composition (Kočišová et al., 2013; Kočišová & Procházka, 2011), thermotropic phase (González-Gutiérrez et al., 2017), or liposome size (Adams et al., 2008).

Naturally, one would try to control this evaporation phenomenon to obtain a more leveled lipid film and reduce the appearance of vesicle defects. In 2018, Mampallil and Eral

reviewed the published methods for CRE suppression (Mampallil & Eral, 2018) and other authors have enlisted known techniques to control solute deposition patterns (Larson, 2012).

It has been established that all CRE suppression protocols rely on at least one of three general strategies: prevention of contact line pinning, disruption of the outward radial flow, and solute trapping. Since we sought for an uncontaminated sample, we were not comfortable with strategies that modify the chemical composition of either the ITO substrate or the liposome suspension.

As an alternative, we are proposing to take advantage of the same outward advective flow that produces the CRE in the first place. This effect will be leveraged in our favor if it applies a leveling shear stress on a previously dried ringlike stain. To this end, we cast progressively bigger liposome droplets on the same spot of an ITO coated electrode, generating a large and smoothed multilayer film.

After characterization of the resulting electroformed samples using optical microscopy, we will compare our multi-droplet technique with the traditional single-droplet method, to look for a statistically significant difference in GUV quality based on the number of vesicle defects.

II.3 Hypothesis

We believe that our proposed technique will be able to significantly decrease the number of vesicle defects in the GUV sample.

II.4 Objective

To develop a straightforward, solvent-free method for the preparation of defect-free GUVs by electroformation.

II.5 Methodology

II.5.1 Materials

The following reagents were purchased in dry powder form from Avanti Polar Lipids (Alabaster, USA):

- 1,2-dimyristoyl-*sn*-glycero-3-phosphocholine (DMPC)

- 1-myristoyl-2-[12-[(7-nitro-2-1,3-benzoxadiazol-4-yl)amino]dodecanoyl]-*sn*-glycero-3-phosphocholine (14:0-12:0 NBD PC)

The following reagents were purchased from Sigma-Aldrich (Toluca, México):

- Chloroform (anhydrous, ≥99%, with 0.5-1.0% ethanol as stabilizer)
- Methanol (anhydrous, 99.8%)
- Sucrose (≥99.5%)
- D-(+)-glucose

Extran MA 02 was purchased from Merck México (Naucalpan de Juárez, México). Sylgard 184 silicone elastomer base and curing agent were purchased from Dow Corning (Midland, USA). Twice distilled water was further deionized with a Milli-Q IQ 7000 Ultrapure Water System from Merck Millipore México (Naucalpan de Juárez, México) before use. ITO coated coverslips (18x18 mm, ~100 Ohm/sq.) were purchased from NANOCS (New York, USA).

II.5.2 Methods

Liposome suspension

DMPC lyophilized powder was weighed in an OHAUS Explorer EX224 analytical balance to prepare an aqueous suspension of unilamellar vesicles (LUVs). The balance was carefully calibrated with the help of a Troemner certified weight set (ID No. 4000017899) before each experiment run.

The weighed lipid was hydrated with 1 mL of deionized water, then vortexed and thermalized at 45 °C (above the phase transition temperature of DMPC). This suspension was extruded for a total of 15 passes through a polycarbonate membrane (30 nm pore size) using a preheated (45 °C) Avanti Mini Extruder. In the case of fluorescence experiments, DMPC powder was doped with 2 mol % of 14:0-12:0 NBD PC before hydration and extrusion. The quality of all the LUV suspensions was monitored by dynamic light scattering (Zetasizer Nano ZS, Malvern).

Substrate cleaning and electrode preparation

Two ITO coated square coverslips were cleaned with Extran MA 02 using a cotton swab and rinsed with deionized water. The ITO coated side of each coverslip was further swabbed with methanol and chloroform before a final DI water rinse. Each cleansed ITO coated coverslip was attached to the center of a round (42 mm diameter) bare glass coverslip using polydimethylsiloxane (Sylgard 184) and left to crosslink at 80 °C for 60 minutes. Finally, a thin strip of copper foil tape was attached to the conductive side of the prepared glass electrode.

Thin film deposition

We performed a preliminary study showing that the ideal liposome concentration for our deposition technique was 50 µg/mL. After dilution, the LUV suspension was loaded into a Hamilton syringe and mounted in a micromanipulator using a 3D printed PLA holder. The fabricated ITO electrode was placed in the motorized stage of an inverted microscope (Axio Observer.Z1, Zeiss).

With this setup, we proceeded to cast three 0.1 µL droplets at equidistant positions on the left side of the ITO coated square coverslip. After complete evaporation, three small ring-like stains of phospholipid material were left on the substrate due to the CRE. As a next step, a new set of three 0.2 µL droplets was placed exactly above the previously dried lipid stains and left to dry as well. The process was iterated using 0.3, 0.4, 0.6, 0.9, 1.2, and 1.6 µL droplets of the same LUV suspension. As a final treatment, pure deionized water was used to serially cast 2.1 and 2.6 µL droplets in the same manner. This protocol results in three separate circular multilayer films containing 265 ng of lipid mass each. For the film deposition controls, three 10 µL droplets (at a concentration of 25.6 µg/mL) were used to cast three separate single-droplet films on the right side of the same ITO coated substrate. This film deposition protocol was designed so that samples and controls would be subjected to the same electroformation conditions simultaneously.

Electroformation chamber and protocol

An electroformation chamber was assembled using a commercially available device suitable for microscopic examination (POC-R2, Pecon). We used the outer frame of this chamber to hold the two facing electrodes with the help of a screw ring and a silicone gasket (1 mm thickness) as spacer (**Figure II.1**). Before assembly, the three lipid film replicates from each

group were hydrated with 15 μL droplets of 50 mM sucrose solution that was preheated to 45 °C. After sandwiching the hydration droplets between the facing electrodes, a function generator was connected to the copper foil strips. Immediately afterwards, an alternating current was applied using a sine wave setting at a 10 Hz frequency and 500 mV as initial voltage. The voltage reached 1 V after an increasing ramp of 20 mV/min and was maintained at this magnitude for 60 min before turning it off. The whole electroformation protocol was executed at a sample temperature of 45 °C using a stage-top incubation system (Incubator PM S1, Insert P S1, Pecon) mounted on the inverted microscope.

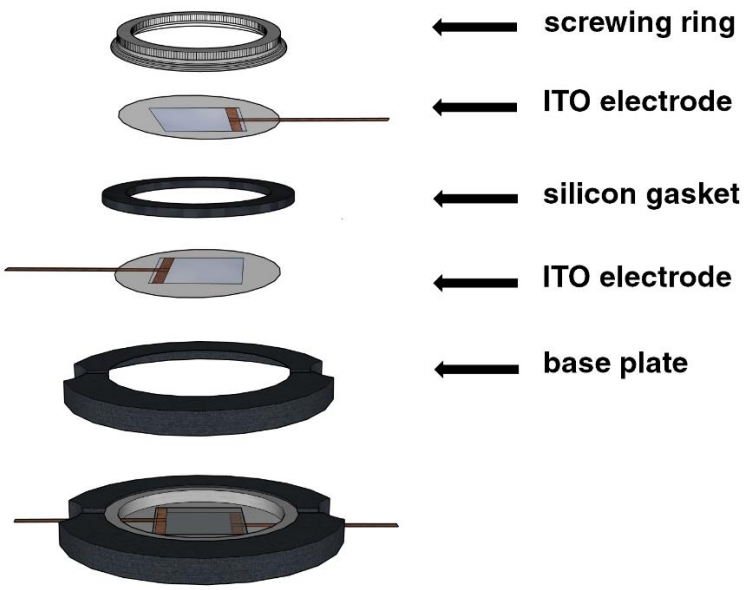

Figure II.1. Schematic representation of the described electroformation chamber both as unassembled parts, as well as an assembled whole below.

GUV detachment and examination

Before detachment, the electroformation chamber was cooled down to 20 °C. GUVs in the phospholipid gel phase are easily detached from the substrate by gentle manual tapping. After detachment, the three replicates from each group (sandwiched droplets on each side of the substrate) were made to coalesce by careful tilting of the chamber. This way, we were left with two larger drops, one from each experimental group, that contained all the detached material in the form of clean GUVs and possible vesicle defects.

Following detachment, the chamber was disassembled, and the sucrose drops were carefully transferred to separate examination cells pre-filled with a 50 mM glucose solution that caused sedimentation of sucrose-filled GUVs. At each experimental run, 150 GUVs were randomly selected from each examination cell, and dual-channel (phase-contrast/fluorescence) photomicrographs were acquired for vesicle characterization. Image processing for lamellarity determination (step fluorescence intensity) was performed according to the validation protocol of (McPhee, Zoriniants, Langbein, & Borri, 2013) using ZEN 2 Pro image software.

II.6 Results and discussion

According to DLS results, our liposome extrusion protocol generates a monodisperse suspension of DMPC LUVs with a Z-average diameter of 64.64 ± 1.65 nm and a small polydispersity index (0.061 ± 0.006). The left column in **Figure II.2** shows a representative image of the ring-like stains that are left after evaporation of the initial droplets in our proposed multi-droplet technique. We fluorescently labeled the LUVs suspension to obtain a relative measurement of the lipid mass distribution in these dried stains.

As expected, after evaporation of a single 0.1 μL droplet, the fluorescence intensity profile reveals an uneven distribution marked by an accumulation of mass at the edge due to the outward flow in the drying droplet. The velocity field describing this flow has already been derived analytically and corroborated using finite element analysis (H. Hu & Larson, 2005b, 2005a). These researchers concluded that the radial velocity in evaporating sessile droplets can reach magnitudes of up to 9-18 μm/s. Assuming a no-slip boundary condition, the axisymmetric radial velocity component should follow a parabolic profile along the vertical axis of the droplet. We hypothesized that the outward shear stress from the gradient of this velocity profile could be strong enough to spread a previously dried lipid ring-like stain, effectively leveraging the CRE hydrodynamics in our favor.

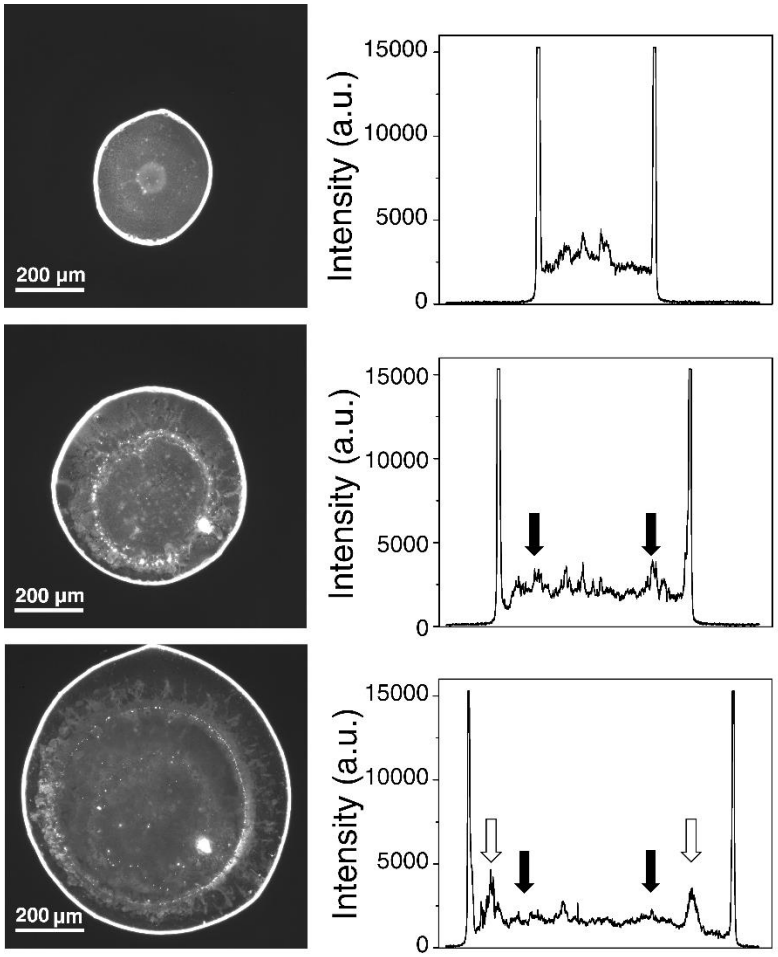

Figure II.2. Fluorescence photomicrographs (left column) of lipid ring-like stains after casting and drying three consecutive droplets of increasing volume (0.1, 0.2, and 0.3 µL) on the same spot of the ITO coated substrate using DMPC liposomes doped with 14:0-12:0 NBD PC (2 mol %); 10x objective, scale bar = 200 µm. Corresponding fluorescence intensity profiles (right column) along the equator of the stains showing their mass distribution; filled and open arrows point to the original position of the first and second rings respectively.

As can be seen from the second and third rows of **Figure II.2**, casting and drying a larger droplet over a previously dried ringlike stain has a leveling effect on the film. Even though the larger droplet leaves a ring on its own, it effectively smears all the previous smaller rings. The two droplets of pure DI water that are used as the final step of our protocol (see **Methodology**) help to finish the ring smearing process without leaving significant rings at their own contact lines.

Our proposed technique could be implemented with serially larger drops to cover as much substrate as desired, but one should consider that evaporation time will increase quadratically with larger droplets (Deegan et al., 2000). A side experiment to test the reproducibility of our droplet volume series resulted in lipid films with a mean area of 8.6 ± 0.2 mm^2 at each casting spot (**Figure II.3**).

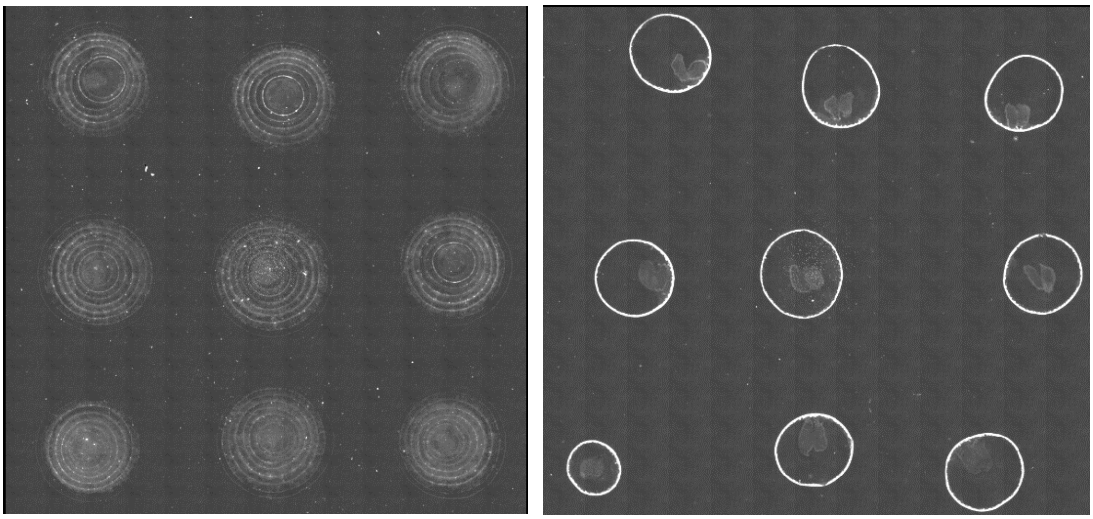

Figure II.3. Mosaics of phase-contrast photomicrographs in 2.5D (where pixel brightness is being represented as height) depicting nine lipid film depositions on an ITO-coated substrate using the proposed drop-casting volume series (left) vs the traditional single-droplet method (right). Both mosaics of images span a total substrate area of 14 mm x 14 mm.

It can be seen from the preceding figure that the dried ringlike stains of the traditional single-droplet method show a brighter signal in phase-contrast microscopy, but also have an increased variability in size and position. One should be aware that the size of the initial liquid-substrate interface, created at the time of droplet impingement on the bare ITO-coated substrate, is usually smaller than the final area of the dried stain. This effect is effectively suppressed with our multi-droplet technique, and contact lines were seen to stop receding whenever droplets were casted over previously dried stains.

Film samples and controls were also subjected to atomic force microscopy (AFM) analysis as dry films. Height fields were obtained using the tapping mode over randomly selected positions on each one of the rings that compose the proposed multi-droplet structure. From each micrograph, root-mean-squared (RMS) roughness was obtained using Gwyddion Open

Source Software and plotted as a function of its corresponding ring. Rings were numbered in the same order than their droplets from the volume series, so that the initial 0.1 μL droplet corresponds to ring number 1. Likewise, the two final 2.1 and 2.6 μL droplets using just DI water instead of liposomes correspond to rings number 9 and 10 respectively (**Figure II.4**). The same procedure was followed in the case of film controls, where we only have one ring due to the single-droplet deposition.

We can see that RMS values are smaller towards the center but also at the periphery of the multi-droplet structure. Central rings were the first to be casted, so they are smeared by all the following droplets of the volume series. On the other hand, rings number 9 and 10 were left by pure DI water droplets, and do not leave a significant accumulation of lipid mass by themselves. Their sole purpose is to continue the smearing process, especially on ring number 8, which is the last one where the liposome suspension is used. Film controls show just a single ringlike stain with an RMS value at least about 3.5 times larger than the ones observed in the multi-droplet structure.

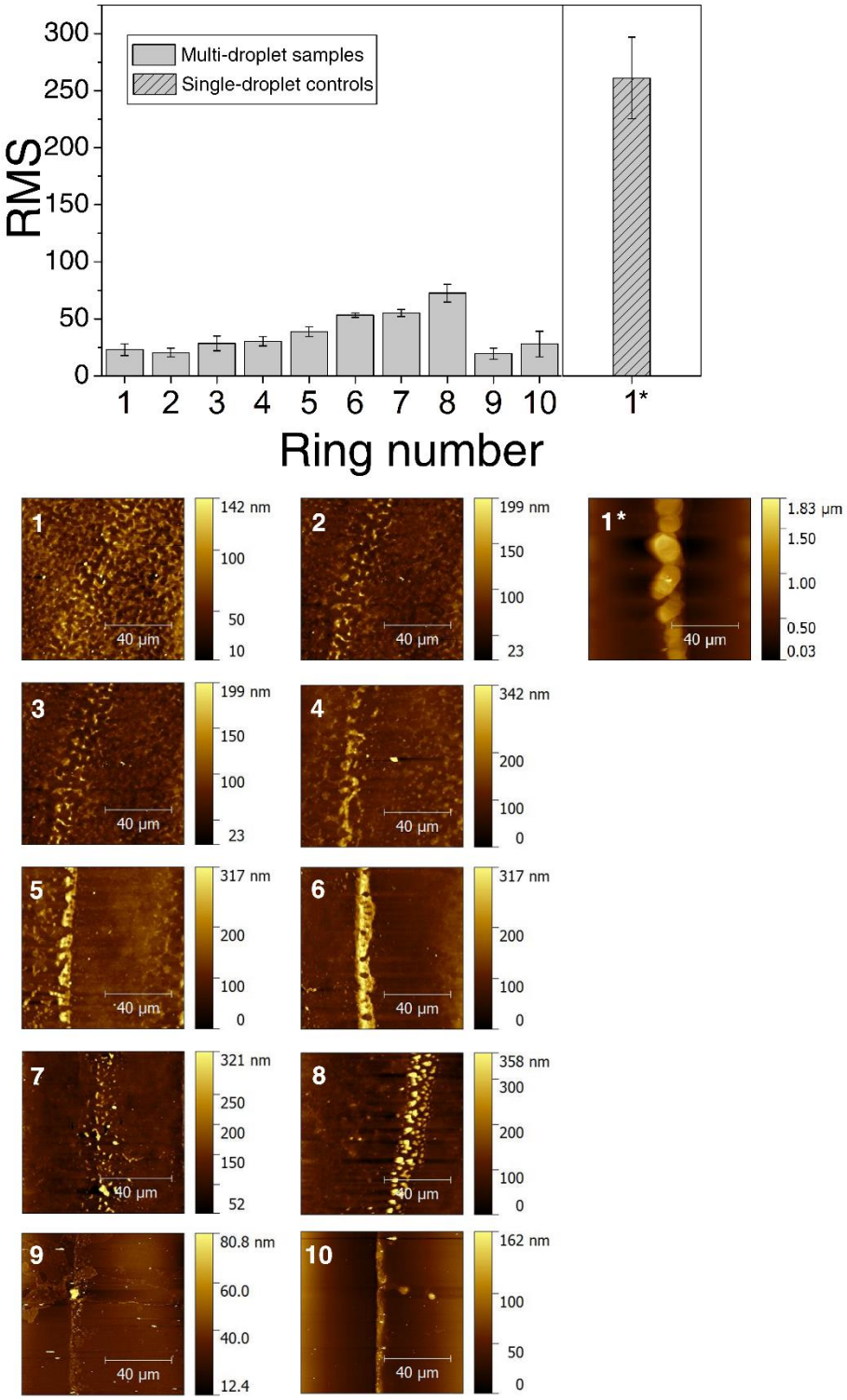

Figure II.4. RMS plots as a function of ring number for both the proposed multi-droplet technique and the traditional single droplet method. Also shown are representative AFM

images corresponding to the obtained height fields from multiple positions in each ring for both lipid film samples and film controls.

We learned that the observed ring smearing effect occurs in three separate stages. During the first stage, the aqueous phase of the newly deposited droplet helps to swell the previously dried lipid stain, giving way to observable multilamellar structures (**Figure II.5 a-b**). Afterwards, when the droplet contact angle is collapsing, a second stage ensues where swollen lipid material is seen to stretch radially following the outward advective flow (**Figure II.5 c-d**). Finally, as the contact line starts to recede, the liquid front drags some of the lipid material towards the center of the stain (**Figure II.5 e-f**).

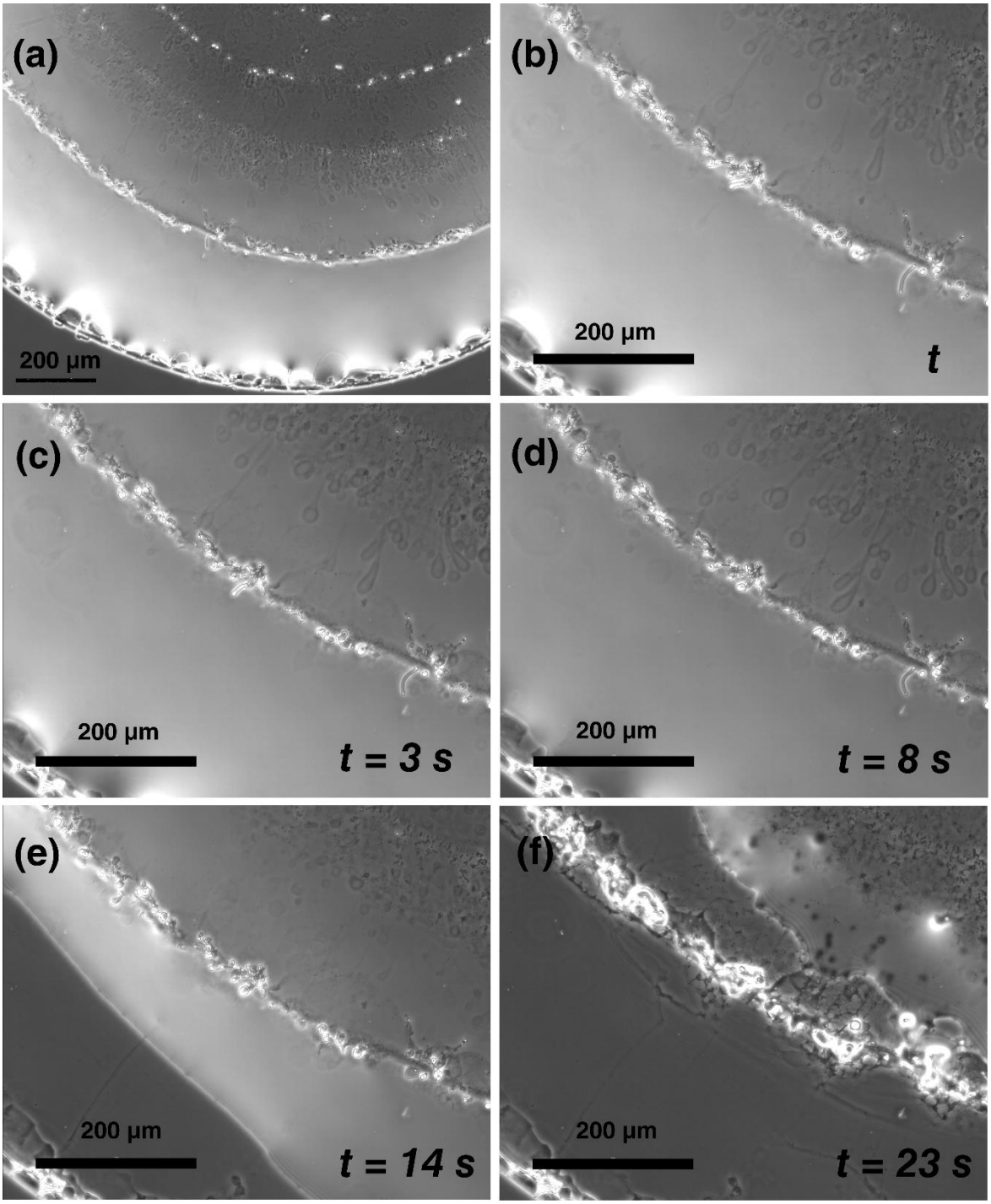

Figure II.5. Phase-contrast micrographs showing three stages of ring-like stain smearing during droplet drying (10x objective, white and black scale bars = 200 µm). The first image (**a**) shows the edge of a large droplet over previously dried stains towards the end of its evaporation (contact line has not started to recede yet). A digitally zoomed-in image (**b**) shows hydrated multilamellar structures underwater. Second and third rows show a time-

lapse series depicting movement of lipid material in an outward stretching phase (**c-d**) and an inward dragging phase (**e-f**). The receding liquid front can be clearly observed in the third row.

Figure II.6 shows the result after lipid film samples and controls were simultaneously subjected to the same electroformation protocol. Electroformed GUVs from each type of film were also subjected to the same detachment conditions (see **Methodology**). Virtually no GUVs with vesicle defects are observed using the proposed multi-droplet technique (**Figure II.6, 1st row**). On the contrary, the uneven lipid distribution of the traditional method produces a characteristic zone at the edge of the film with numerous vesicle defects (**Figure II.6, 2nd row**). Rodriguez et al. had previously quantified the electroformation defect rate to be as high as 20% and calculated that ~25% of the original lipid material was found in defects (Rodriguez et al., 2005). If one tries to use a much lower concentration of liposome suspension hoping to reduce the vesicle defects at the single-droplet film edge, a "barren" central zone will be obtained where the lipid film did not have enough bilayers to produce GUVs successfully.

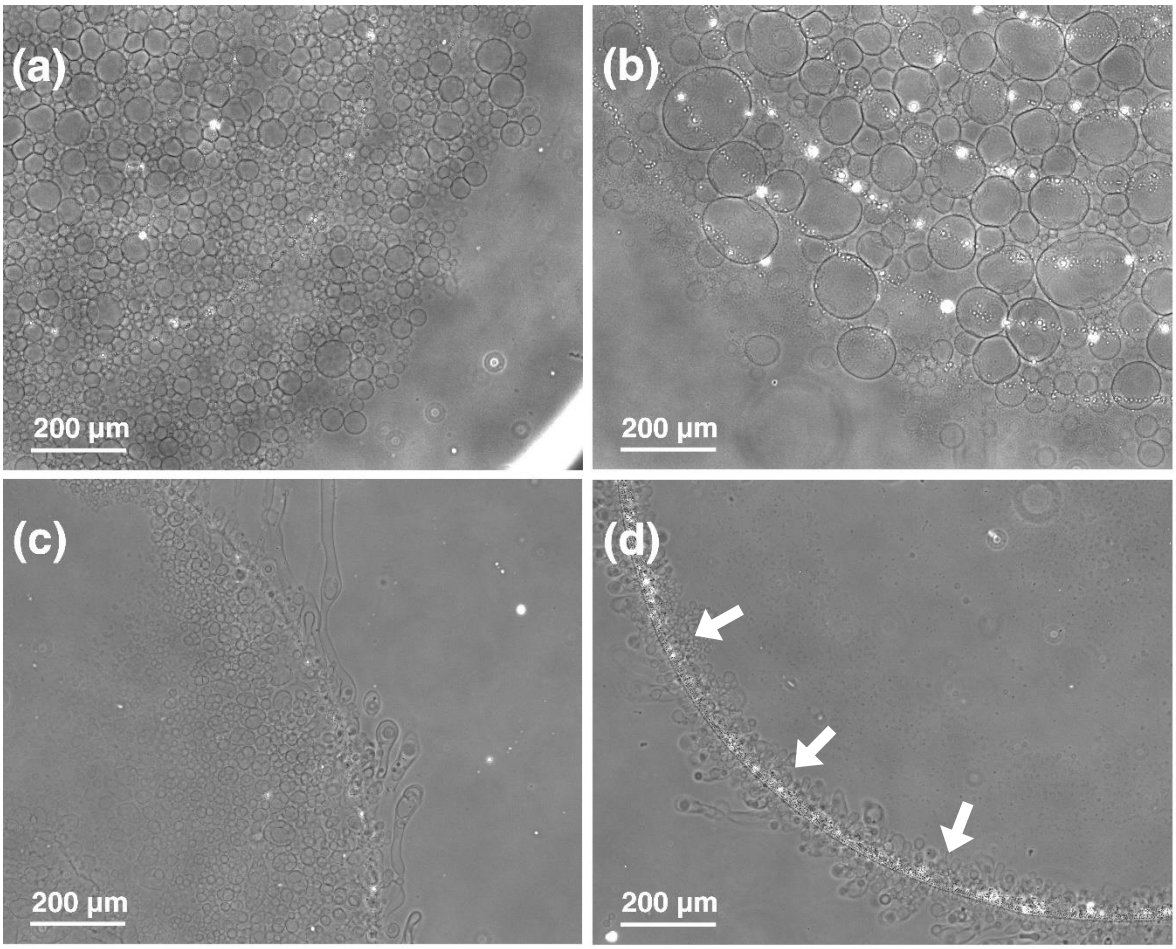

Figure II.6. Phase-contrast micrographs showing electroformed GUVs still attached to the ITO-coated electrodes using both the traditional and the proposed technique (10x objective, scale bars = 200 µm). (a) Using a smoothened multilayer film produces a high number of defect-free GUVs spanning the whole lipid film. (b) Defect-free GUVs can grow to surpass 100 µm in diameter if electroformation time is prolonged. (c) Using the same lipid mass to deposit a single-drop film generates many vesicle defects at the edge of the film (white arrows). (d) If the lipid concentration of the deposition is reduced a "barren zone" appears towards the central part of the film.

Figure II.7 shows the characterization of electroformation products from five runs of the multi-droplet film deposition experiment vs. single-droplet controls. Although there is no difference between the average diameter of electroformed GUVs, there is a dramatic reduction in the proportion of all types of lipid defects. The most common defects were multivesicular vesicles (MVV), where GUVs are seen to contain one or more vesicles inside.

Multilamellar vesicles (MLV) are those with more than one bilayer on their wall but a sub-optical inter-bilayer separation. Lipid tethers and vesicles that deviated from sphericity were grouped in the less frequent class of defects, the non-spherical vesicles (NSV). **Figure II.8** shows representative images of detached vesicles and their lamellarity distributions using each technique. Vesicle defect rate in the control group agrees with previous reports (Rodriguez et al., 2005). On the contrary, samples using the proposed technique showed defects in less than 1% of the analyzed GUV population.

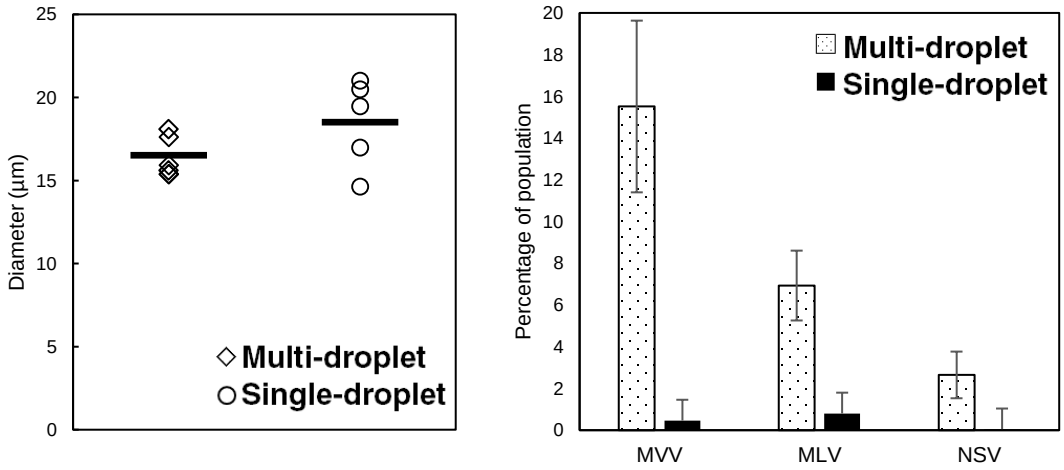

Figure II.7. (a) Diamonds show the average vesicle diameter for each run (n = 150 at each run) of the multi-droplet deposition experiment and circles do the same for single-casting controls, horizontal bars indicate global averages in each experimental group. **(b)** Percentage of the analyzed GUV population (n = 150 at each run) showing mutually exclusive classes of lipid defects (MVV = multivesicular vesicles, MLV = multilamellar vesicles, NSV = non-spherical vesicles), error bars show the standard deviation of the mean in 5 runs.

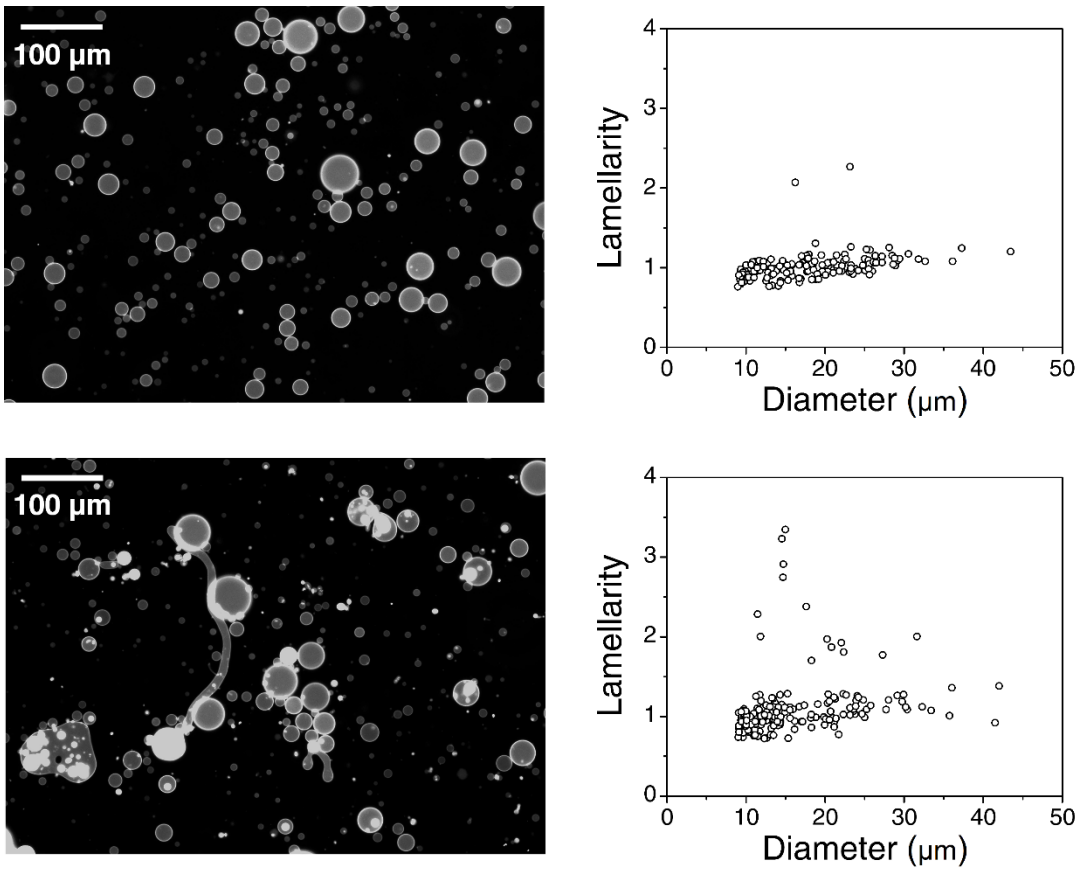

Figure II.8. Left. Fluorescence micrographs showing detached and sedimented GUVs from the multi-droplet films **(top)** vs. single-droplet deposition **(bottom)** (10x objective, scale bars = 100 µm). **Right.** Lamellarity distribution for the analyzed GUV population from each technique, circles show normalized step intensities from the central zone of each GUV. See reference (McPhee et al., 2013) for further details on lamellarity determination.

II.7 Conclusion

The challenge of controlling the deposition of molecules with self-organizing properties like phospholipids is readily recognized in the literature (Le Berre et al., 2009). In our search for lipid film evenness we chose to take advantage of the microflow hydrodynamics of the drying sessile droplet to construct a multi-droplet self-leveled deposition technique that uses a minimal quantity of lipid material.

Clean GUVs are reproducibly generated using just a fraction of the lipid material reported on previous protocols that also employ liposomes to prepare lipid films (Baykal-

Caglar, Hassan-Zadeh, Saremi, & Huang, 2012; Bhatia et al., 2015; Pott et al., 2008). Our method could be readily exploited when GUVs are prepared using precious lipid material like gangliosides or phosphatidylinositols.

Furthermore, it is a solvent-free and straightforward solution to virtually eliminate vesicle defects that does not require specialized equipment or elaborate setups. We believe that our protocol could be further optimized by automatization using tools like inkjet printing with variable-sized droplet technology. Perhaps it may find its way into other research tools where an uneven deposition is undesirable, such as polynucleotide or protein microarrays (Malainou, Petrou, Kakabakos, Gogolides, & Tserepi, 2012).

Chapter III. The influence of cardiolipin on phase-separated lipid mixtures.

We took advantage of the optimized setup developed in the previous chapter to explore lipid-lipid interactions in microscopically explorable model membranes (GUVs). As will be seen in this chapter, lipid interactions in the context of domain formation and phase separation of lipid mixtures is still a subject of debate and several hypotheses have been put forward. We explore this subject experimentally in the remaining section of this thesis.

III.1 Introduction

In 1997, Kai Simons made a dent into the theory of biological membranes when he and Elina Ikonen proposed their lipid raft hypothesis (Simons & Ikonen, 1997). Back then, the role of lipids in cellular membrane function was limited to that of a solvent for membrane proteins as a result of the established fluid mosaic model (Singer & Nicolson, 1972). Simons challenged this idea after the observation of key asymmetries in the lipid matrix of these membranes.

Besides the clear distinction between an exoplasmic and a cytoplasmic lipidome, they suggested a potential structure in the bidimensional plane of the membrane. This lateral organization would be the result of a preferential association between sphingolipids (glycosphingolipids and sphingomyelin), cholesterol and so-called "raft proteins" like glycosylphosphatidylinositol (GPI)-anchored proteins but also acylated kinases, cholesterol-binding caveolin, and transmembrane proteins. They posed a picture where these microdomains would serve two principal purposes:

- To act as sorting domains in the Golgi for the differential transport of selected membrane-interacting molecules
- Once placed in their targeted membranes, to serve as relay stations for membrane-interacting molecules effectively coupling events on the outside of the cell with signaling pathways inside of it.

Simons recognized that this picture depended on the presence of lipid species with mostly saturated chains in both leaflets to create a relatively ordered phase with high molecular density where cholesterol could act as a "spacer" to fill the voids in the raft bilayer. These voids are a consequence of the raft lipidome, which is characterized by asymmetric acyl chains, and voluminous headgroups (Simons & Ikonen, 1997).

After more than a decade of the initial proposal and over 10,000 citations on his original article, different researchers have both supported and rejected the model. Supporters have suggested involvement of raft microdomains in a wide array of cellular functions including apoptosis, cytoskeleton organization, synaptic transmission, cell adhesion and migration, and exo or endocytosis. As well as functioning as the point of entry of different pathogens into the eukaryotic cell. Researchers that reject the model have argued that the traditional detection methods for the existence of these microdomains (i.e. resistance to detergent solubilization, and sensitivity to cholesterol depletion) are indirect and potentially artifactual. Additionally, *in vivo* studies that have provided evidence for local clustering report widely varying values (25-700 nm) for the size of membrane domains (Munro, 2003).

Simons himself has published more than one personal account describing his point of view in the debate. Both parties recognize that membrane models of fluid-fluid coexistence have provided an important framework for understanding the biophysical mechanisms that contribute to biomembrane heterogeneity. Thanks to the advancement in microscopic and spectroscopic techniques, there is now plausible evidence for cellular membrane subcompartmentalization (Lingwood & Simons, 2010). The modern consensus is that lipid rafts are small (nanoscale) and highly dynamic (fluctuating) sterol and sphingolipid-enriched domains. Such domains may stabilize and form larger platforms after specific "activating" interactions. This new conception of "lipid rafts" is very different from a well-defined phase separated at equilibrium (Pike, 2006).

Nanoscale organization is not an unknown phenomenon in pure lipid biophysics. The most obvious example is the modulated ripple phase $P_{\beta'}$, which shows that even single lipid systems can possess ~10 nm periodicities that have been characterized by atomic force microscopy measurements (Leidy, Kaasgaard, Crowe, Mouritsen, & Jørgensen, 2002). Binary mixtures of phosphatidylcholines and cholesterol have also been shown to show cholesterol-induced fluid-phase immiscibility producing nanoscale fluctuating domains (Sankaram & Thompson, 1991).

It is only in ternary mixtures of a low melting lipid, a high melting lipid, and cholesterol, where macroscopic phase separation has readily been identified (Veatch & Keller, 2003). However, some of these ternary systems (deemed type I mixtures by Feigenson) only show

nanodomain formation, but how is this possible? How is it that type I ternary systems can circumvent the free energy penalty associated with the large amount of interdomain interface in the bilayer plane? Different theories can be found in the literature.

Keller & Veatch proposed that nanoscale fluctuations are manifestations of critical behavior in the membrane system (Veatch & Keller, 2005). Criticality is characterized by clusters of an average size that is set by the correlation length of a radially averaged correlation function. As the critical point is approached, the correlation length diverges. These researchers proposed that even when the miscibility temperature of biological membranes is well below the physiological, lipid composition is nonetheless critical, and the correlation length at physiological temperature is within the same nanoscale order than the putative rafts *in vivo*.

They have also showed that membrane behavior is indeed critical it will belong to the universality class of the two-dimensional Ising model; and the correlation length ξ, the line tension λ, and the width of isothermal tie lines Δc within the miscibility gap all follow established power law predictions ($\xi \propto |T - T_c|^{-1}$, $\lambda \propto |T - T_c|$, and $\Delta c \sim |T - T_c|^{1/8}$). An important caveat of this theory is that when free lipid membranes are coupled to cortical cytoskeleton proteins, critical behavior is no longer supported, and the model is best represented by the two dimensional random-field Ising model where macroscopic phase separation is always suppressed (Imry & Ma, 1975).

Another theory puts forward the idea that lipids can be segregated based on elastic properties like bending moduli or spontaneous curvature. In this case small liquid ordered domains could be stabilized by an interplay between their boundary energy (i.e. line tension) and their bending energy (J. Hu, Weikl, & Lipowsky, 2011). This means that for sufficiently low line tension, lipid rafts could be present if the liquid ordered domains had a positive spontaneous curvature. In this case lipid rafts will be more like dimples with smaller interface perimeters than their flat counterparts. The alternative would be a highly fluctuating membrane where flat but "stiff" lipid rafts are prevented to coalesce due to curvature-imposed coarsening barriers. Unfortunately, line tension values should be way below those reported for typical phase separating mixtures (Amazon, Goh, & Feigenson, 2013).

Supported membranes of phase separating mixtures that are subjected to stripped patterns in the supporting substrate, show alignment of liquid ordered domains with low-curvature regions of the pattern. This observation would speak in favor of a domain stabilization process where the bending modulus of liquid ordered phases is too high and line tension cannot induce domain coarsening past "virtual fences" of elevated curvature (Parthasarathy, Yu, & Groves, 2006)

A slightly different scenario for curvature-coupled composition is the Leibler-Andelman mechanism. Lipids with a non-zero spontaneous curvature could segregate in anticorrelated alternate domains between the two leaflets of the bilayer if there is enough lateral tension that keeps the bilayer planar on average. This theory is suggesting that ordered domains are not in registry with ordered domains in the opposing monolayer, a fact that is contrary to some biophysical experiments (Collins & Keller, 2008).

The preceding theories establish a potential physical basis for the stabilization of nanoscale domains that otherwise would have merged given the appropriate system conditions. But what about systems that do not show true phase separation and still have structural order that differs from complete randomness in composition? These systems are called microemulsions and show rapidly decaying autocorrelation functions (Cornell et al., 2018). This could be a plausible basis to explain parallel domains in the cytoplasmic leaflet where the lipidome is composed of unsaturated phosphatidylserines, phosphatidylethanolamines and no sphingolipids (Tian-yun Wang & Silvius, 2001).

For the case of microemulsion stabilization, a mean-field (neglected fluctuations) hypothesis proposes the existence of line active molecules (linactants) that could reduce the energy penalty of interface formation by aggregating at domain boundaries. In this framework, there is a threshold linactant concentration at which line tension vanishes and a modulated phase appears. The modulated phase is conceived as an intermediate state between macroscopic and nanoscopic domain formation (Goh, Amazon, & Feigenson, 2013). Explored candidates for the putative membrane linactant include hybrid lipids (unsaturation in only one acyl chain), but also cholesterol (Tsai & Feigenson, 2019).

An interesting theory conciliating an exoplasmic leaflet that could phase separate, with a cytoplasmic leaflet that could not, has been put forward by Schick. His theoretical work proposes a scenario where lateral order is initially induced on the inner leaflet due to height fluctuations segregating phosphatidylethanolamine domains from phosphatidylserine/cholesterol domains due to the spontaneous curvature of the former. Spontaneous curvature of PE is negative and around five times larger in magnitude than the small positive curvature of PS. This segregation would stabilize a composition-curvature coupled microemulsion that could easily induce lateral order in the exoplasmic leaflet thanks either to its critical composition or to the actual existence of an exoplasmic linactant (Shlomovitz & Schick, 2013). The order propagation to the outer leaflet could be mediated by cholesterol or by interdigitating SM species. This model has been tested theoretically with plausible results (Sadeghi, Müller, & Vink, 2014).

III.2 Justification

The Schick model seems very attractive due to the added fact that internal domains enriched in PS would create an effective transduction platform, especially for second messengers like protein kinase C (PKC). All of PKC subclasses require phosphatidylserine for their activation (Newton, 1997). In biological membranes, the intermonolayer asymmetry that ensures an inner leaflet rich in PS and PE, is actively maintained by special proteins named flippases, and floppases (Hankins, Baldridge, Xu, & Graham, 2015). This means that in order to test Schick's hypothesis in a protein-free model membrane we need a species that fulfills two key characteristics:

- Has a large spontaneous curvature.
- Selectively partitions into the inner monolayer.

Cardiolipin is a complex lipid with a large packing parameter, double negative charge and a large negative spontaneous curvature (-1.1 nm^{-1} CL vs -0.3 nm^{-1} in PE), which has been known to selectively localize in bacterial membranes and mitochondrial cristae. It is composed of linked phosphatidic acids covalently attached by a glycerol moiety and it is now known that can form self-associating clusters (thanks to an attractive CL-CL interaction parameter) which partition into inner leaflets of model membranes. Moreover, estimates for the cluster size from these attractive interactions is in the same nanoscale than putative

cellular rafts, making CL the perfect lipid species to test Schick's hypothesis (Beltrán-Heredia et al., 2019).

We could then design an experiment to include cardiolipin in well-studied phase-separated ternary systems. This lipid species could act both as a curvature inducing molecule, as well as a putative linactant. In the former scenario, the appearance of a modulated phase will also depend on the parallel existence of intermonolayer coupling. Schick proposes that the most likely candidate for intermonolayer coupling is cholesterol. The molecule shows a thermodynamic preference for PS and SM inducing order of their acyl chains and possible interdigitation. In the later scenario, perhaps the CL molecule helps reduce the tension created by hydrophobic mismatch between liquid ordered and liquid disordered phases.

III.3 Hypothesis

The Schick model posits a phase diagram where a macroscopic modulated phase forms if the temperature is lowered. It is in this context that we want to test whether or not a clear modulated phase appears in phase-separated ternary systems after addition of tetramyristoil-phosphatidylcholine (TMCL) at different molar fractions.

III.4 Objective

We are looking to provide a piece of evidence that supports or rejects the Schick model where a microemulsion can be induced by curvature-coupled composition heterogeneities in a model membrane.

III.5 Methodology

III.5.1 Materials

The following reagents were purchased in dry powder form from Avanti Polar Lipids (Alabaster, USA):

- 1,2-dipalmitoyl-*sn*-glycero-3-phosphocholine (DPPC)
- 1,2-dioleoyl-*sn*-glycero-3-phosphocholine (DOPC)
- Cholesterol (ovine wool, >98%)
- 1',3'-bis[1,2-dimyristoyl-*sn*-glycero-3-phospho]-glycerol (sodium salt) (TMCL)

- 1,2-dipalmitoyl-*sn*-glycero-3-phosphoethanolamine-N-(7-nitro-2-1,3-benzoxadiazol-4-yl) (ammonium salt) (16:0 NBD PE)

1,2-dihexadecanoyl-*sn*-glycero-3-phosphoethanolamine, (triethylammonium salt) (Texas Red DHPE) was purchased from Thermo Fischer Scientific. Chloroform (anhydrous, ≥99%, with 0.5-1.0% ethanol as stabilizer), methanol (anhydrous, 99.8%), sucrose (≥99.5%), and D-(+)-glucose were from Sigma-Aldrich México.

Extran MA 02 was purchased from Merck México (Naucalpan de Juárez, México). Sylgard 184 silicone elastomer base and curing agent were purchased from Dow Corning (Midland, USA). Twice distilled water was further deionized with a Milli-Q IQ 7000 Ultrapure Water System from Merck Millipore México (Naucalpan de Juárez, México) before use. ITO coated coverslips (18x18 mm, ~100 Ohm/sq.) were purchased from NANOCS (New York, USA).

III.5.2 Methods

Liposome suspension

Lipid lyophilized powders including fluorescent probes were weighed in the desired proportions using an OHAUS Explorer EX224 analytical balance to prepare an organic solvent solution in 2:1 $CHCl_3$/MeOH. The balance was carefully calibrated with the help of a Troemner certified weight set (ID No. 4000017899) before each experiment run.

After stirring at 60 °C and subsequent solvent removal in vacuum, the mixed lipid film was hydrated with 1 mL of deionized water, then vortexed and thermalized at 60 °C (above the phase transition temperature of the highest melting lipid in the mixture). This suspension was extruded for a total of 15 passes through a polycarbonate membrane (30 nm pore size) using a preheated (60 °C) Avanti Mini Extruder. The quality of all the LUV suspensions was monitored by dynamic light scattering (Zetasizer Nano ZS, Malvern) and the final suspension was diluted to 50 µg/mL before use.

Substrate cleaning and electrode preparation

Two ITO coated square coverslips were cleaned with Extran MA 02 using a cotton swab and rinsed with deionized water. The ITO coated side of each coverslip was further swabbed

with methanol and chloroform before a final DI water rinse. Each cleansed ITO coated coverslip was attached to the center of a round (42 mm diameter) bare glass coverslip using polydimethylsiloxane (Sylgard 184) and left to crosslink at 80 °C for 60 minutes. Finally, a thin strip of copper foil tape was attached to the conductive side of the prepared glass electrode.

Thin film deposition

After dilution, the LUV suspension was loaded into a Hamilton syringe and mounted in a micromanipulator using a 3D printed PLA holder. The fabricated ITO electrode was placed in the motorized stage of an inverted microscope (Axio Observer.Z1, Zeiss). With this setup, we proceeded prepare sample (DPPC/DOPC/Chol/TMCL 0.36:0.36:0.18:0.10 mol%) and control (DPPC/DOPC/Chol 0.40:0.40:0.20 mol%) multilayer films using our developed protocol (see **Chapter II**). Both sample and control mixtures were doped with 1 mol% 16:0 NBD PE that selectively partitions into the liquid-ordered phase, and also 1 mol% Texas Red DHPE that selectively partitions into the liquid-disordered phase.

Electroformation chamber and protocol

An electroformation chamber was assembled using a commercially available device suitable for microscopic examination (POC-R2, Pecon). We used the outer frame of this chamber to hold the two facing electrodes with the help of a screw ring and a silicone gasket (1 mm thickness) as spacer (**Figure II.1**). Before assembly, the three lipid film replicates from each group were hydrated with 15 μL droplets of 50 mM sucrose solution that was preheated to 60 °C. After sandwiching the hydration droplets between the facing electrodes, a function generator was connected to the copper foil strips. Immediately afterwards, an alternating current was applied using a sine wave setting at a 10 Hz frequency and 500 mV as initial voltage. The voltage reached 1 V after an increasing ramp of 20 mV/min and was maintained at this magnitude for 60 min before turning it off. The whole electroformation protocol was executed at a sample temperature of 60 °C using a stage-top incubation system (Incubator PM S1, Insert P S1, Pecon) and an IR lamp, both mounted on the inverted microscope.

GUV detachment and examination

Before detachment, the electroformation chamber was cooled down to 25 °C and GUVs were detached from the substrate by gentle manual tapping. After detachment, the three replicates

from each group (sandwiched droplets on each side of the substrate) were made to coalesce by careful tilting of the chamber. This way, we were left with two larger drops, one from each experimental group.

Following detachment, the chamber was disassembled, and the sucrose drops were carefully transferred to separate examination cells pre-filled with a 50 mM glucose solution that caused sedimentation of sucrose-filled GUVs. At each experimental run, GUVs were randomly selected from each examination cell, and dual-channel (NBD/Texas Red) fluorescence photomicrographs were acquired for vesicle characterization. Image processing was performed using ZEN 2 Pro image software.

III.6 Results and discussion

The DPPC/DOPC/Chol ternary mixture (**Figure III.6**) is well-known to produce macroscopic phase separation at a 2:2:1 molar ratio (Veatch & Keller, 2003). The miscibility transition temperature is defined as the one where 50% of GUVs show fluid-fluid coexistence. In our setup, miscibility temperature for controls was observed at 34.6 ± 0.3 °C.

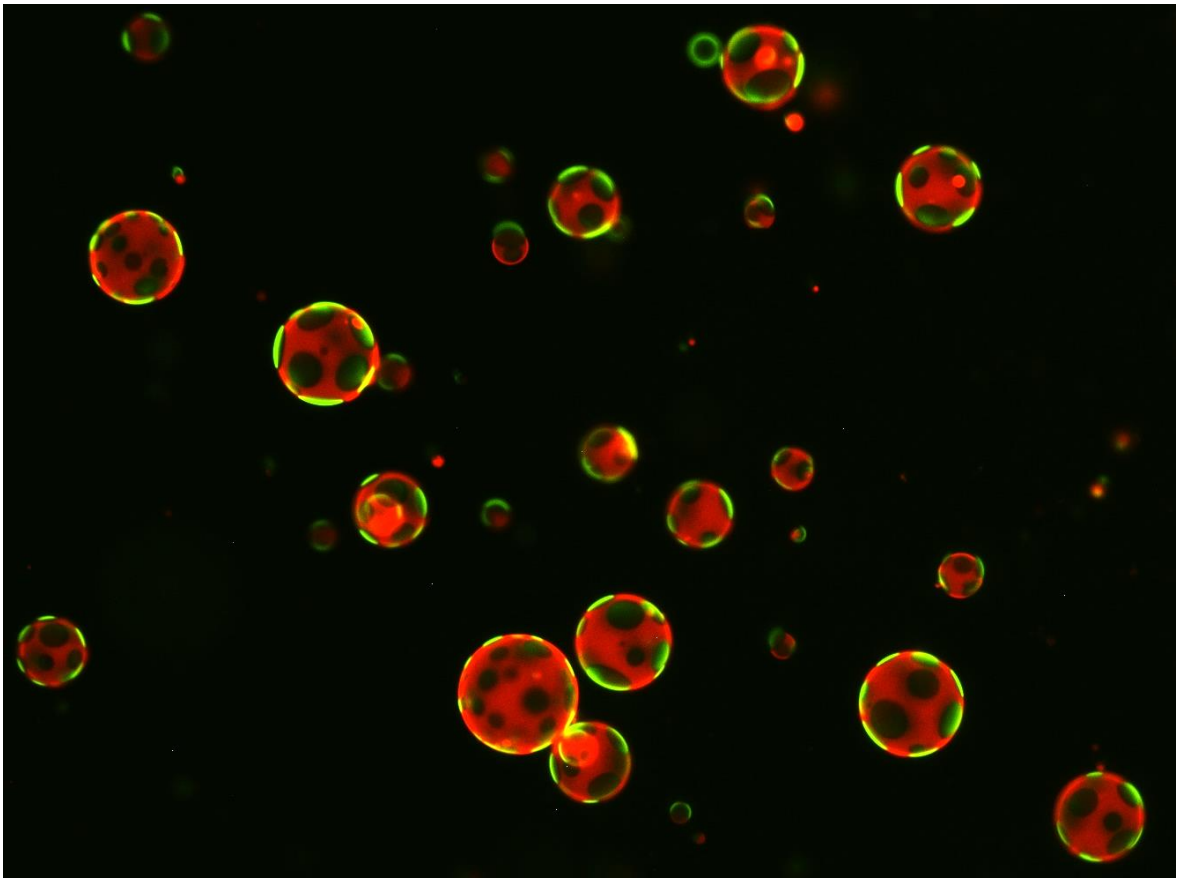

Figure III.1 Optical fluorescence photomicrographs showing sucrose filled GUVs with the control lipid mixture DPPC/DOPC/Chol 0.40:0.40:0.20, sedimented in glucose solution. Phase separation and coarsening of liquid-ordered domains before complete equilibrium is readily observed.

Traditional model systems that mimic CL-containing biomembranes use a 10% molar concentration of this lipid (Khalifat, Fournier, Angelova, & Puff, 2011). After addition of this species to the mixtures (**Figure III.2**), fluid-fluid coexistence was apparently suppressed, and replaced by small and amorphous or stripped domains that do not seem to diffuse or change shape freely and neither show coarsening after time.

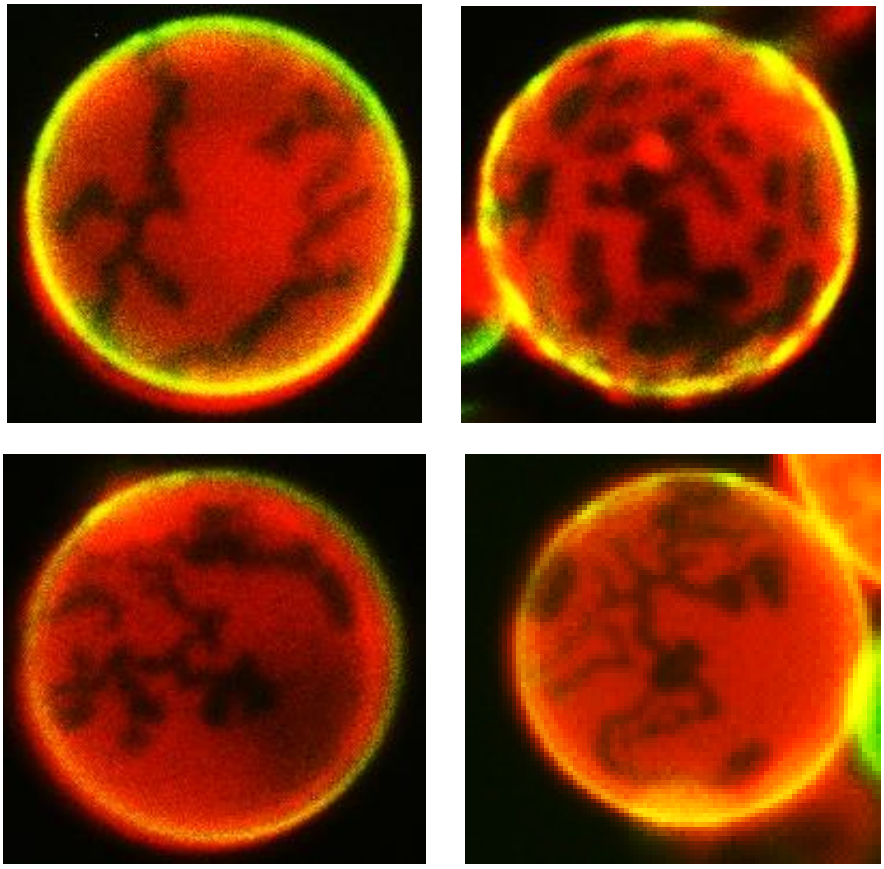

Figure III.2 Optical fluorescence photomicrographs showing sucrose filled GUVs with the sample lipid mixture DPPC/DOPC/Chol/TMCL 0.36:0.36:0.18:0.10, sedimented in glucose solution. Phase separation in the form of circular liquid ordered domains is seen to be replaced by stripped and "fixed" domain formation.

Due to the settings of our electroformation protocol, sucrose solution originally prepared at 50 mM tends to increase its concentration due to mild evaporation during the application of the alternating voltage. After GUV detachment, the vesicles tend to be subjected to an hypoosmotic shock because glucose-filled exploration cells have a 50 mM concentration. This scenario increases the osmotic tension in the vesicles, so that the majority of GUVs are quite tense during exploration.

An elevated tension in the vesicle bilayer would naturally suppress height fluctuations, making it impossible to observe the appearance of a true modulated phase due to curvature-coupled phase separation. We would need to subject the vesicles to a slightly more hypertonic batch and explore their behavior in that setting.

We do see however, the existence of amorphous and/or stripped domains that have a much larger domain interface than the one observed in liquid circular domains or clumped gel domains from the DPPC/DOPC system (see **Figure III.3**). This fact would suggest a lower line tension after the addition of CL, perhaps supporting its role as an effective linactant.

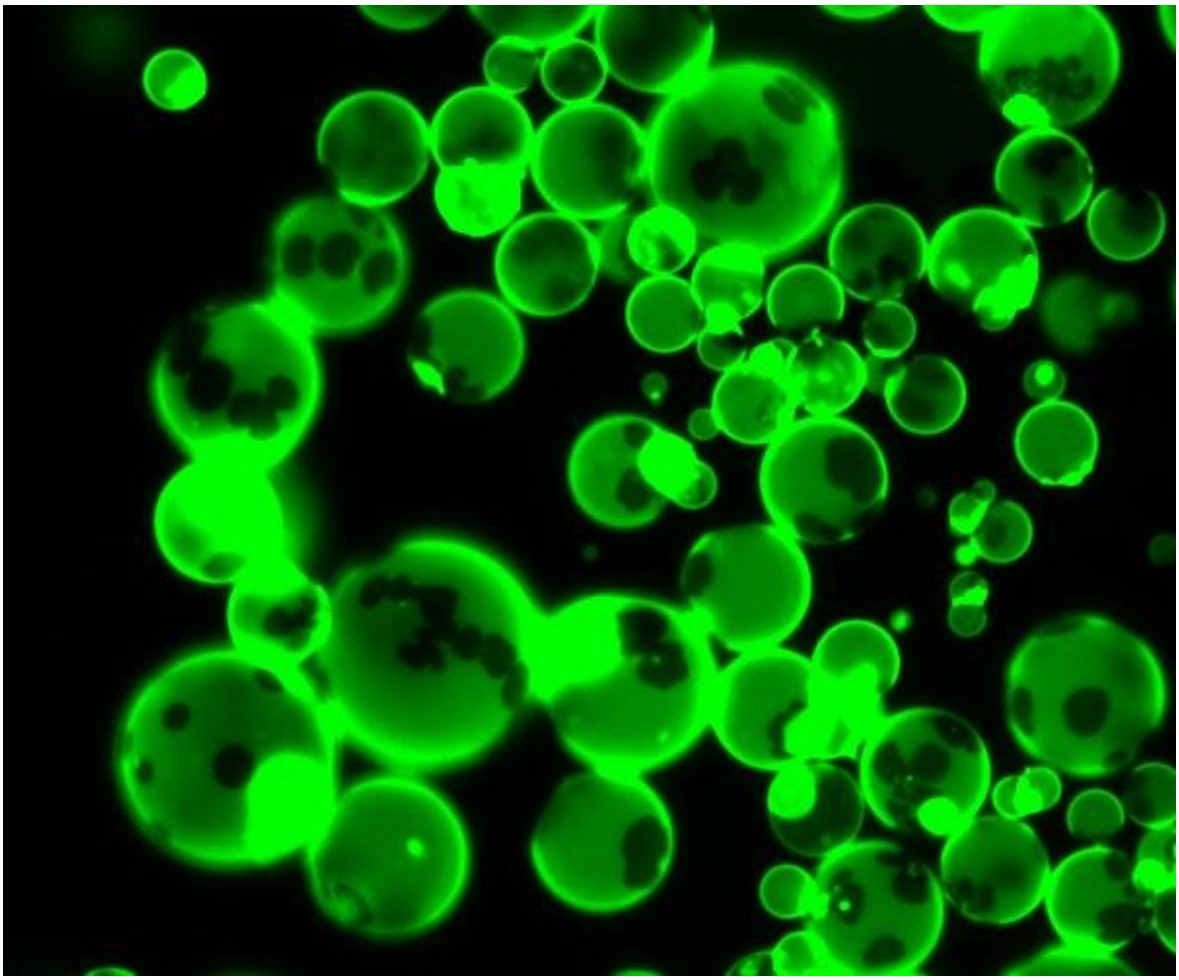

Figure III.3 Optical fluorescence photomicrographs showing sucrose filled GUVs with a lipid mixture of DPPC/DOPC 0.5:0.5, sedimented in glucose solution. Gel-fluid coexistence is observed in the form of irregular and non-coalescing domains.

Previous studies have shown both experimentally and theoretically that increasing membrane tension reduces miscibility temperatures, suppressing phase-separation at temperatures where macroscopic domains are usually observed (Portet, Gordon, & Keller, 2012) (Uline, Schick, & Szleifer, 2012). However, conflicting results are also observed when

GUVs are subjected to parallel increased osmotic pressure (Oglęcka, Rangamani, Liedberg, Kraut, & Parikh, 2014) (Hamada, Kishimoto, Nagasaki, & Takagi, 2011).

This conflict prompts us even further to explore the impact of our sample mixture in the case of non-tense membranes. In fact, Schick's hypothesis results in a characteristic size of the fluctuations in composition of the form $(\kappa/\sigma)^{1/2}$ for a bending rigidity κ and a membrane tension σ (Schick, 2012).

III.7 Conclusion

Based on the lipidome of the mammalian plasma membrane, Schick's hypothesis presents a plausible framework to understand both bilayer asymmetry and the appearance of dynamic composition fluctuations as the physical basis for lipid rafts. Curvature-composition coupling would allow intermonolayer communication to take place effectively and endow the membrane with its original purpose of biological signaling relay. We saw that the addition of 10 mol% CL is able to suppress fluid-fluid coexistence in favor of stripped and amorphous domains with much longer phase boundaries and hence lower line tension.

The exploration of the effect of some other thermodynamic parameters like membrane tension and osmotic pressure would perhaps uncover a true modulated phase in the ternary system. Likewise, pseudoternary mixtures that include SM would permit us to explore the behavior of interdigitating lipid species in this context. Finally, the implication of ions cannot be neglected, since all of our experiments were performed with deionized water only.

References

Adams, D. R., Toner, M., & Langer, R. (2008). Microflow and Crack Formation Patterns in Drying Sessile Droplets of Liposomes Suspended in Trehalose Solutions. *Langmuir, 24*(15), 7688–7697. https://doi.org/10.1021/la703835w

Akbarzadeh, A., Rezaei-Sadabady, R., Davaran, S., Joo, S. W., Zarghami, N., Hanifehpour, Y., … Nejati-Koshki, K. (2013). Liposome: classification, preparation, and applications. *Nanoscale Research Letters*, *8*(1), 102. https://doi.org/10.1186/1556-276X-8-102

Almeida, P. F. (2011). A Simple Thermodynamic Model of the Liquid-Ordered State and the Interactions between Phospholipids and Cholesterol. *Biophysical Journal*, *100*(2), 420–429. https://doi.org/10.1016/j.bpj.2010.12.3694

Almeida, P. F. F. (2009). Thermodynamics of lipid interactions in complex bilayers. *Biochimica et Biophysica Acta (BBA) - Biomembranes*, *1788*(1), 72–85. https://doi.org/10.1016/j.bbamem.2008.08.007

Almeida, P. F. F., Vaz, W. L. C., & Thompson, T. E. (1992). Lateral diffusion in the liquid phases of dimyristoylphosphatidylcholine/cholesterol lipid bilayers: a free volume analysis. *Biochemistry*, *31*(29), 6739–6747. https://doi.org/10.1021/bi00144a013

Amazon, J. J., Goh, S. L., & Feigenson, G. W. (2013). Competition between line tension and curvature stabilizes modulated phase patterns on the surface of giant unilamellar vesicles: A simulation study. *Physical Review E*, *87*(2), 022708. https://doi.org/10.1103/PhysRevE.87.022708

Angelova, M. I., & Dimitrov, D. S. (1986). Liposome electroformation. *Faraday Discussions of the Chemical Society*, *81*, 303. https://doi.org/10.1039/dc9868100303

Antonietti, M., & Förster, S. (2003). Vesicles and Liposomes: A Self-Assembly Principle Beyond Lipids. *Advanced Materials*, *15*(16), 1323–1333. https://doi.org/10.1002/adma.200300010

B'Hymer, C. (2003). Residual solvent testing: a review of gas-chromatographic and alternative techniques. *Pharmaceutical Research*, *20*(3), 337–344. https://doi.org/10.1023/A:1022693516409

Bagatolli, L. a, Parasassi, T., & Gratton, E. (2000). Giant phospholipid vesicles: comparison among the whole lipid sample characteristics using different preparation methods: a two photon fluorescence microscopy study. *Chemistry and Physics of Lipids*, *105*(2), 135–147. Retrieved from http://www.ncbi.nlm.nih.gov/pubmed/10823462

Bangham, A. D. (1968). Membrane models with phospholipids. *Progress in Biophysics and Molecular Biology*, *18*, 29–95. https://doi.org/10.1016/0079-6107(68)90019-9

Bartelt, S. M., Steinkühler, J., Dimova, R., & Wegner, S. V. (2018). Light-Guided Motility of a Minimal Synthetic Cell. *Nano Letters*, *18*(11), 7268–7274. https://doi.org/10.1021/acs.nanolett.8b03469

Batzri, S., & Korn, E. D. (1973). Single bilayer liposomes prepared without sonication. *Biochimica et Biophysica Acta (BBA) - Biomembranes*, *298*(4), 1015–1019. https://doi.org/10.1016/0005-2736(73)90408-2

Baykal-Caglar, E., Hassan-Zadeh, E., Saremi, B., & Huang, J. (2012). Preparation of giant

unilamellar vesicles from damp lipid film for better lipid compositional uniformity. *Biochimica et Biophysica Acta*, *1818*(11), 2598–2604. https://doi.org/10.1016/j.bbamem.2012.05.023

Beltrán-Heredia, E., Tsai, F.-C., Salinas-Almaguer, S., Cao, F. J., Bassereau, P., & Monroy, F. (2019). Membrane curvature induces cardiolipin sorting. *Communications Biology*, *2*(1), 225. https://doi.org/10.1038/s42003-019-0471-x

Bhatia, T., Husen, P., Brewer, J., Bagatolli, L. A., Hansen, P. L., Ipsen, J. H., & Mouritsen, O. G. (2015). Preparing giant unilamellar vesicles (GUVs) of complex lipid mixtures on demand: Mixing small unilamellar vesicles of compositionally heterogeneous mixtures. *Biochimica et Biophysica Acta - Biomembranes*, *1848*(12), 3175–3180. https://doi.org/10.1016/j.bbamem.2015.09.020

Brunner, J., Skrabal, P., & Hausser, H. (1976). Single bilayer vesicles prepared without sonication physico-chemical properties. *Biochimica et Biophysica Acta (BBA) - Biomembranes*, *455*(2), 322–331. https://doi.org/10.1016/0005-2736(76)90308-4

Capello, C., Fischer, U., & Hungerbühler, K. (2007). What is a green solvent? A comprehensive framework for the environmental assessment of solvents. *Green Chemistry*, *9*(9), 927. https://doi.org/10.1039/b617536h

Charcosset, C., El-Harati, A., & Fessi, H. (2005). Preparation of solid lipid nanoparticles using a membrane contactor. *Journal of Controlled Release*, *108*(1), 112–120. https://doi.org/10.1016/j.jconrel.2005.07.023

Clarke, C. J., Tu, W.-C., Levers, O., Bröhl, A., & Hallett, J. P. (2018). Green and Sustainable Solvents in Chemical Processes. *Chemical Reviews*, *118*(2), 747–800. https://doi.org/10.1021/acs.chemrev.7b00571

Collins, M. D., & Keller, S. L. (2008). Tuning lipid mixtures to induce or suppress domain formation across leaflets of unsupported asymmetric bilayers. *Proceedings of the National Academy of Sciences*, *105*(1), 124–128. https://doi.org/10.1073/pnas.0702970105

Cornell, C. E., Skinkle, A. D., He, S., Levental, I., Levental, K. R., & Keller, S. L. (2018). Tuning Length Scales of Small Domains in Cell-Derived Membranes and Synthetic Model Membranes. *Biophysical Journal*, *115*(4), 690–701. https://doi.org/10.1016/j.bpj.2018.06.027

Cortesi, R., Esposito, E., Gambarin, S., Telloli, P., Menegatti, E., & Nastruzzi, C. (1999). Preparation of liposomes by reverse-phase evaporation using alternative organic solvents. *Journal of Microencapsulation*, *16*(2), 251–256. https://doi.org/10.1080/026520499289220

Deegan, R. D. (2000). Pattern formation in drying drops. *Physical Review E*, *61*(1), 475–485. https://doi.org/10.1103/PhysRevE.61.475

Deegan, R. D., Bakajin, O., Dupont, T. F., Huber, G., Nagel, S. R., & Witten, T. A. (1997). Capillary flow as the cause of ring stains from dried liquid drops. *Nature*, *389*(6653), 827–829. https://doi.org/10.1038/39827

Deegan, R. D., Bakajin, O., Dupont, T. F., Huber, G., Nagel, S. R., & Witten, T. A. (2000). Contact line deposits in an evaporating drop. *Physical Review E*, *62*(1), 756–765. https://doi.org/10.1103/PhysRevE.62.756

Dervichian, D. G. (1964). The physical chemistry of phospholipids. *Progress in Biophysics and Molecular Biology*, *14*, 263-IN3. https://doi.org/10.1016/S0079-6107(64)80008-0

Deshpande, S., & Dekker, C. (2018). On-chip microfluidic production of cell-sized liposomes. *Nature Protocols*, *13*(5), 856–874. https://doi.org/10.1038/nprot.2017.160

Dwivedi, A. M. (2002). Residual solvent analysis in pharmaceuticals. *Pharmaceutical Technology*, *133*(November), 42–46. Retrieved from http://www.pharmtech.com/pharmtech/article/articleDetail.jsp?id=57607

Estes, D. J., & Mayer, M. (2005). Electroformation of giant liposomes from spin-coated films of lipids. *Colloids and Surfaces B: Biointerfaces*, *42*(2), 115–123. https://doi.org/10.1016/j.colsurfb.2005.01.016

Goh, S. L., Amazon, J. J., & Feigenson, G. W. (2013). Toward a Better Raft Model: Modulated Phases in the Four-Component Bilayer, DSPC/DOPC/POPC/CHOL. *Biophysical Journal*, *104*(4), 853–862. https://doi.org/10.1016/j.bpj.2013.01.003

González-Gutiérrez, J., Pérez-Isidoro, R., Pérez-Camacho, M. I., & Ruiz-Suárez, J. C. (2017). The calorimetric properties of liposomes determine the morphology of dried droplets. *Colloids and Surfaces B: Biointerfaces*, *155*, 215–222. https://doi.org/10.1016/j.colsurfb.2017.04.022

Guida, V. (2010). Thermodynamics and kinetics of vesicles formation processes. *Advances in Colloid and Interface Science*, *161*(1–2), 77–88. https://doi.org/10.1016/j.cis.2009.11.004

Haberland, M. E., & Reynolds, J. a. (1973). Self-association of Cholesterol in Aqueous Solution. *Proceedings of the National Academy of Sciences*, *70*(8), 2313–2316. https://doi.org/10.1073/pnas.70.8.2313

Hamada, T., Kishimoto, Y., Nagasaki, T., & Takagi, M. (2011). Lateral phase separation in tense membranes. *Soft Matter*, *7*(19), 9061. https://doi.org/10.1039/c1sm05948c

Hankins, H. M., Baldridge, R. D., Xu, P., & Graham, T. R. (2015). Role of Flippases, Scramblases and Transfer Proteins in Phosphatidylserine Subcellular Distribution. *Traffic*, *16*(1), 35–47. https://doi.org/10.1111/tra.12233

Heimburg, T. (2007). *Thermal Biophysics of Membranes*. *Zhurnal Eksperimental'noi i Teoreticheskoi Fiziki*. Weinheim, Germany: Wiley-VCH Verlag GmbH & Co. KGaA. https://doi.org/10.1002/9783527611591

Helm, C., Israelachvili, J., & McGuiggan, P. (1989). Molecular mechanisms and forces involved in the adhesion and fusion of amphiphilic bilayers. *Science*, *246*(4932), 919–922. https://doi.org/10.1126/science.2814514

Horváth, I. T. (2018). Introduction: Sustainable Chemistry. *Chemical Reviews*, *118*(2), 369–371. https://doi.org/10.1021/acs.chemrev.7b00721

Hu, H., & Larson, R. G. (2005a). Analysis of the Effects of Marangoni Stresses on the Microflow in an Evaporating Sessile Droplet. *Langmuir*, *21*(9), 3972–3980. https://doi.org/10.1021/la0475270

Hu, H., & Larson, R. G. (2005b). Analysis of the Microfluid Flow in an Evaporating Sessile Droplet. *Langmuir*, *21*(9), 3963–3971. https://doi.org/10.1021/la047528s

Hu, J., Weikl, T., & Lipowsky, R. (2011). Vesicles with multiple membrane domains. *Soft Matter*, *7*(13), 6092. https://doi.org/10.1039/c0sm01500h

Huang, J., Buboltz, J. T., & Feigenson, G. W. (1999). Maximum solubility of cholesterol in phosphatidylcholine and phosphatidylethanolamine bilayers. *Biochimica et Biophysica Acta (BBA) - Biomembranes*, *1417*(1), 89–100. https://doi.org/10.1016/S0005-2736(98)00260-0

Imry, Y., & Ma, S. (1975). Random-Field Instability of the Ordered State of Continuous Symmetry. *Physical Review Letters*, *35*(21), 1399–1401. https://doi.org/10.1103/PhysRevLett.35.1399

Khalifat, N., Fournier, J.-B., Angelova, M. I., & Puff, N. (2011). Lipid packing variations induced by pH in cardiolipin-containing bilayers: The driving force for the cristae-like shape instability. *Biochimica et Biophysica Acta (BBA) - Biomembranes*, *1808*(11), 2724–2733. https://doi.org/10.1016/j.bbamem.2011.07.013

Kočišová, E., Antalík, A., & Procházka, M. (2013). Drop coating deposition Raman spectroscopy of liposomes: role of cholesterol. *Chemistry and Physics of Lipids*, *172–173*, 1–5. https://doi.org/10.1016/j.chemphyslip.2013.04.002

Kočišová, E., Petr, M., Šípová, H., Kylián, O., & Procházka, M. (2017). Drop coating deposition of a liposome suspension on surfaces with different wettabilities: "coffee ring" formation and suspension preconcentration. *Physical Chemistry Chemical Physics*, *19*(1), 388–393. https://doi.org/10.1039/C6CP07606H

Kočišová, E., & Procházka, M. (2011). Drop-coating deposition Raman spectroscopy of liposomes. *Journal of Raman Spectroscopy*, *42*(8), 1606–1610. https://doi.org/10.1002/jrs.2915

Krisovitch, S. M., & Regen, S. L. (1992). Nearest-neighbor recognition in phospholipid membranes: a molecular-level approach to the study of membrane suprastructure. *Journal of the American Chemical Society*, *114*(25), 9828–9835. https://doi.org/10.1021/ja00051a015

Larson, R. G. (2012). Re-Shaping the Coffee Ring. *Angewandte Chemie International Edition*, *51*(11), 2546–2548. https://doi.org/10.1002/anie.201108008

Le Berre, M., Chen, Y., & Baigl, D. (2009). From Convective Assembly to Landau−Levich Deposition of Multilayered Phospholipid Films of Controlled Thickness. *Langmuir*, *25*(5), 2554–2557. https://doi.org/10.1021/la803646e

Lee, K. Y., Park, S., Lee, K. A., Kim, S.-H., Kim, H., Meroz, Y., … Shin, K. (2018). Photosynthetic artificial organelles sustain and control ATP-dependent reactions in a protocellular system. *Nature Biotechnology*, *36*(6), 530–535. https://doi.org/10.1038/nbt.4140

Leidy, C., Kaasgaard, T., Crowe, J. H., Mouritsen, O. G., & Jørgensen, K. (2002). Ripples and the Formation of Anisotropic Lipid Domains: Imaging Two-Component Supported Double Bilayers by Atomic Force Microscopy. *Biophysical Journal*, *83*(5), 2625–2633. https://doi.org/10.1016/S0006-3495(02)75273-9

Lindblom, G., Orädd, G., & Filippov, A. (2006). Lipid lateral diffusion in bilayers with phosphatidylcholine, sphingomyelin and cholesterol. *Chemistry and Physics of Lipids*, *141*(1–2), 179–184. https://doi.org/10.1016/j.chemphyslip.2006.02.011

Lingwood, D., & Simons, K. (2010). Lipid Rafts As a Membrane-Organizing Principle. *Science*,

327(5961), 46–50. https://doi.org/10.1126/science.1174621

Malainou, A., Petrou, P. S., Kakabakos, S. E., Gogolides, E., & Tserepi, A. (2012). Creating highly dense and uniform protein and DNA microarrays through photolithography and plasma modification of glass substrates. *Biosensors and Bioelectronics*, *34*(1), 273–281. https://doi.org/10.1016/j.bios.2012.02.020

Mampallil, D., & Eral, H. B. (2018). A review on suppression and utilization of the coffee-ring effect. *Advances in Colloid and Interface Science*, *252*, 38–54. https://doi.org/10.1016/j.cis.2017.12.008

Marsh, D. (2013). *Handbook of Lipid Bilayers, Second Edition*. *European journal of biochemistry* (Vol. 59). CRC Press. https://doi.org/10.1201/b11712

McPhee, C. I., Zoriniants, G., Langbein, W., & Borri, P. (2013). Measuring the Lamellarity of Giant Lipid Vesicles with Differential Interference Contrast Microscopy. *Biophysical Journal*, *105*(6), 1414–1420. https://doi.org/10.1016/j.bpj.2013.07.048

Mozafari, M. R., Reed, C. J., Rostron, C., Kocum, C., & Piskin, E. (2002). Construction of stable anionic liposome-plasmid particles using the heating method: a preliminary investigation. *Cellular & Molecular Biology Letters*, *7*(3), 923–927. Retrieved from http://www.cmbl.org.pl

Munro, S. (2003). Lipid Rafts. *Cell*, *115*(4), 377–388. https://doi.org/10.1016/S0092-8674(03)00882-1

Newton, A. C. (1997). Regulation of protein kinase C. *Current Opinion in Cell Biology*, *9*(2), 161–167. https://doi.org/10.1016/S0955-0674(97)80058-0

Nishimura, K., Matsuura, T., Nishimura, K., Sunami, T., Suzuki, H., & Yomo, T. (2012). Cell-Free Protein Synthesis inside Giant Unilamellar Vesicles Analyzed by Flow Cytometry. *Langmuir*, *28*(22), 8426–8432. https://doi.org/10.1021/la3001703

Oglęcka, K., Rangamani, P., Liedberg, B., Kraut, R. S., & Parikh, A. N. (2014). Oscillatory phase separation in giant lipid vesicles induced by transmembrane osmotic differentials. *ELife*, *3*, 1–18. https://doi.org/10.7554/eLife.03695.001

Ohta-Iino, S., Pasenkiewicz-Gierula, M., Takaoka, Y., Miyagawa, H., Kitamura, K., & Kusumi, A. (2001). Fast Lipid Disorientation at the Onset of Membrane Fusion Revealed by Molecular Dynamics Simulations. *Biophysical Journal*, *81*(1), 217–224. https://doi.org/10.1016/S0006-3495(01)75693-7

Oropeza-Guzman, E., & Ruiz-Suárez, J. C. (2018). Dehydration/Rehydration Cycles for Mixing Phospholipids without the Use of Organic Solvents. *Langmuir*, *34*(23), 6869–6873. https://doi.org/10.1021/acs.langmuir.8b00799

Otake, K., Imura, T., Sakai, H., & Abe, M. (2001). Development of a New Preparation Method of Liposomes Using Supercritical Carbon Dioxide. *Langmuir*, *17*(13), 3898–3901. https://doi.org/10.1021/la010122k

Parthasarathy, R., Yu, C., & Groves, J. T. (2006). Curvature-Modulated Phase Separation in Lipid Bilayer Membranes. *Langmuir*, *22*(11), 5095–5099. https://doi.org/10.1021/la060390o

Patil, Y. P., & Jadhav, S. (2014). Novel methods for liposome preparation. *Chemistry and Physics of Lipids*, *177*, 8–18. https://doi.org/10.1016/j.chemphyslip.2013.10.011

Pike, L. J. (2006). Rafts defined: a report on the Keystone symposium on lipid rafts and cell function. *Journal of Lipid Research*, *47*(7), 1597–1598. https://doi.org/10.1194/jlr.E600002-JLR200

Portet, T., Gordon, S. E., & Keller, S. L. (2012). Increasing Membrane Tension Decreases Miscibility Temperatures; an Experimental Demonstration via Micropipette Aspiration. *Biophysical Journal*, *103*(8), L35–L37. https://doi.org/10.1016/j.bpj.2012.08.061

Pott, T., Bouvrais, H., & Méléard, P. (2008). Giant unilamellar vesicle formation under physiologically relevant conditions. *Chemistry and Physics of Lipids*, *154*(2), 115–119. https://doi.org/10.1016/j.chemphyslip.2008.03.008

Rideau, E., Dimova, R., Schwille, P., Wurm, F. R., & Landfester, K. (2018). Liposomes and polymersomes: a comparative review towards cell mimicking. *Chemical Society Reviews*, *47*(23), 8572–8610. https://doi.org/10.1039/C8CS00162F

Rideau, E., Wurm, F. R., & Landfester, K. (2019). Self-Assembly of Giant Unilamellar Vesicles by Film Hydration Methodologies. *Advanced Biosystems*, *1800324*, 1800324. https://doi.org/10.1002/adbi.201800324

Rodriguez, N., Pincet, F., & Cribier, S. (2005). Giant vesicles formed by gentle hydration and electroformation: A comparison by fluorescence microscopy. *Colloids and Surfaces B: Biointerfaces*, *42*(2), 125–130. https://doi.org/10.1016/j.colsurfb.2005.01.010

Sadeghi, S., Müller, M., & Vink, R. L. C. (2014). Raft Formation in Lipid Bilayers Coupled to Curvature. *Biophysical Journal*, *107*(7), 1591–1600. https://doi.org/10.1016/j.bpj.2014.07.072

Sankaram, M. B., & Thompson, T. E. (1991). Cholesterol-induced fluid-phase immiscibility in membranes. *Proceedings of the National Academy of Sciences*, *88*(19), 8686–8690. https://doi.org/10.1073/pnas.88.19.8686

Schick, M. (2012). Membrane heterogeneity: Manifestation of a curvature-induced microemulsion. *Physical Review E*, *85*(3), 031902. https://doi.org/10.1103/PhysRevE.85.031902

Shlomovitz, R., & Schick, M. (2013). Model of a Raft in Both Leaves of an Asymmetric Lipid Bilayer. *Biophysical Journal*, *105*(6), 1406–1413. https://doi.org/10.1016/j.bpj.2013.06.053

Silvius, J. R. (1986). Solid- and liquid-phase equilibria in phosphatidylcholine / phosphatidylethanolamine mixtures. A calorimetric study. *Biochimica et Biophysica Acta (BBA) - Biomembranes*, *857*(2), 217–228. https://doi.org/10.1016/0005-2736(86)90350-0

Simons, K., & Ikonen, E. (1997). Functional rafts in cell membranes. *Nature*, *387*(6633), 569–572. https://doi.org/10.1038/42408

Singer, S. J., & Nicolson, G. L. (1972). The Fluid Mosaic Model of the Structure of Cell Membranes. *Science*, *175*(4023), 720–731. https://doi.org/10.1126/science.175.4023.720

Tabaei, S. R., Gillissen, J. J. J., Kim, M. C., Ho, J. C. S., Liedberg, B., Parikh, A. N., & Cho, N.-J. (2016). Brownian Dynamics of Electrostatically Adhering Small Vesicles to a Membrane Surface Induces Domains and Probes Viscosity. *Langmuir*, *32*(21), 5445–5450. https://doi.org/10.1021/acs.langmuir.6b00985

Tsai, W.-C., & Feigenson, G. W. (2019). Lowering line tension with high cholesterol content induces a transition from macroscopic to nanoscopic phase domains in model biomembranes.

Biochimica et Biophysica Acta (BBA) - Biomembranes, *1861*(2), 478–485. https://doi.org/10.1016/j.bbamem.2018.11.010

Uline, M. J., Schick, M., & Szleifer, I. (2012). Phase Behavior of Lipid Bilayers under Tension. *Biophysical Journal*, *102*(3), 517–522. https://doi.org/10.1016/j.bpj.2011.12.050

Vaz, W. L. C., Clegg, R. M., & Hallmann, D. (1985). Translational diffusion of lipids in liquid crystalline phase phosphatidylcholine multibilayers. A comparison of experiment with theory. *Biochemistry*, *24*(3), 781–786. https://doi.org/10.1021/bi00324a037

Veatch, S. L., & Keller, S. L. (2003). Separation of Liquid Phases in Giant Vesicles of Ternary Mixtures of Phospholipids and Cholesterol. *Biophysical Journal*, *85*(5), 3074–3083. https://doi.org/10.1016/S0006-3495(03)74726-2

Veatch, S. L., & Keller, S. L. (2005). Seeing spots: Complex phase behavior in simple membranes. *Biochimica et Biophysica Acta (BBA) - Molecular Cell Research*, *1746*(3), 172–185. https://doi.org/10.1016/j.bbamcr.2005.06.010

Walde, P., Cosentino, K., Engel, H., & Stano, P. (2010). Giant Vesicles: Preparations and Applications. *ChemBioChem*, *11*(7), 848–865. https://doi.org/10.1002/cbic.201000010

Wang, Tian-yun, & Silvius, J. R. (2001). Cholesterol Does Not Induce Segregation of Liquid-Ordered Domains in Bilayers Modeling the Inner Leaflet of the Plasma Membrane. *Biophysical Journal*, *81*(5), 2762–2773. https://doi.org/10.1016/S0006-3495(01)75919-X

Wang, Tingting, Ingram, C., & Weisshaar, J. C. (2010). Model Lipid Bilayer with Facile Diffusion of Lipids and Integral Membrane Proteins. *Langmuir*, *26*(13), 11157–11164. https://doi.org/10.1021/la101046r

Witzany, G. (2016). Crucial steps to life: From chemical reactions to code using agents. *Biosystems*, *140*, 49–57. https://doi.org/10.1016/j.biosystems.2015.12.007

Wydro, P. (2011). The interactions between cholesterol and phospholipids located in the inner leaflet of humane erythrocytes membrane (DPPE and DPPS) in binary and ternary films—The effect of sodium and calcium ions. *Colloids and Surfaces B: Biointerfaces*, *82*(1), 209–216. https://doi.org/10.1016/j.colsurfb.2010.08.041